Functionalised porous silicon as a biosensor: Emphasis on monitoring cells in vivo and in vitro

Author:
Gupta, B; Zhu, Y; Guan, B; Reece, PJ; Gooding, JJ

Publication details:
Analyst
v. 138
Chapter No. 13
Medium: Print
pp. 3593 - 3615
0003-2654 (ISSN); 1364-5528 (ISSN)

Publication Date:
2013

Publisher DOI:
https://doi.org/10.1039/c3an00081h

Porous Silicon as an ideal optofluidics material for biosensing: Emphasis on microfabrication and monitoring cells in vivo and in vitro

Bakul Gupta,*[a] Ying Zhu,[a] Bin Guan,[a] Peter J. Reece,[b] J. Justin Gooding*[a]

[a] *School of Chemistry and Australian Centre for NanoMedicine, The University of New South Wales, Sydney, NSW 2052, Australia*
[b] *School of Physics, The University of New South Wales, Sydney, NSW 2052, Australia.*
E-mail: justin.gooding@unsw.edu.au; Fax: +61-2-9385 5384; Tel: +61-2-9385 6141

Porous silicon photonics is the ideal platform for high sensitivity, high selectivity monitoring of biological molecules in a complex fluidic environment. The potential of this technology was identified almost 15 years ago, however, it has taken considerable advances in porous silicon surface chemistry, photonics, and microfabrication to create truly effective devices that can provide new insights into the behaviour of biological systems. In this review we provide a critical assessment of the development of porous silicon optical biosensors from the early demonstrations of affinity based sensing to the current trends in monitoring single cell activity and perspectives in the use of photonic microparticles for biomedical applications.

1. Introduction

Porous silicon (PSi) as a material was first discovered in 1956 but really only attracted significant interest from the 1990s onwards because of discoveries that PSi could photoluminescence,[1] could be fabricated into photonic crystals[2] and had potential as a tunable biomaterial.[3] The combination of the optical properties of PSi, and its potential to be a biocompatible material, quickly saw it begun to be explored as a biosensing material. The first example of a PSi-based biosensor was by Lin *et al.* [4] who took a single layer mesoporous PSi thin film and modified the surface with silane chemistry to allow the attachment of antibodies, ligands or DNA. The ligand attachment was to ensure proteins in solution selectively bound to the surface whilst the modification of the PSi with single strands of DNA enabled the detection of complementary strands of DNA. These PSi devices allow the monitoring of these binding reactions by a change in the average refractive index of the PSi structure, due to biological material binding to the pore walls of the PSi and replacing lower refractive index water that would otherwise be in the pores. The result was a shift in the optical signature of the photonic crystal. Thus in many ways, PSi-based biosensors are the archetypal optofluidic device, and certainly one class of optofluidic devices that have been extensively studied.

The seminal paper by Lin *et al.* [4] is so important not just because it stimulated a large research field, but also because it outlines the potential and challenges in using PSi as an optofluidic device. This first paper showed that PSi could be used as a refractive index based biosensor, that surface chemistry was pivotal in determining the performance of the device, that many types of biosensors could be developed with this one transducing material and PSi was nondestructive to the biological environment being sensed. Since this seminal paper, much work has been done in 1) the development of more sophisticated optical structures made from PSi for biosensing,[5, 6] 2) developing surface chemistries suitable for PSi modification for biosensing applications, [6-8] 3) applying PSi to a range of different biosensing applications,[9, 10] 4) the fabrication of PSi into microstructures and microparticles[11] and 5) the application *in vivo* and in cell biology.[12, 13] This review will focus on such developments in the application of PSi as an optofluidic material for biosensing. As the first three areas of development of using PSi in biosensing have previously been covered in other reviews,[6] this review will cover the first three areas with regards to recent developments before concentrating on the fabrication of PSi into microscale arrays and patterns, as well as the fabrication of microparticles, with a view to using PSi in microfluidics and applying PSi biosensors for cell biology and the potential for *in vivo* applications.

2. Fabricating PSi into Optical Structures

The potential for PSi to function as a refractive index based optical biosensor is possible through its capacity to be structured at both the biomolecular and optical size-scales. Judicious choice of structuring on both scales can be used to independently optimize both the 'bio-recognition interface' and 'optical transducer' components for maximum sensitivity and efficacy. Flexibility in controlling optical properties, compatibility with microfabrication-based processing, and an ability to create truly high quality optical structures, means that a range of different photonic architectures can be implemented depending on the intended sensing application.

The material itself is a monolithic crystalline structure that is perforated with an interconnected matrix of nanometer-sized pores, and is typically formed by anodisation of a silicon wafer in an electrolytic solution containing hydrofluoric acid.[14] PSi forms under galvanostatic conditions at an applied current density that is below the critical value for electropolishing at a constant rate. During the process p-type electrical doping of the substrate provides an excess of positive carriers (holes) that are consumed when the fluoride ions react with the silicon, liberating hydrogen gas in the process and leaving behind voids in the substrate.[15] The reaction progresses at the Si / PSi interface

leaving the previously etched film unaltered. In the absence of holes as majority carriers, such as is the case in n-type doping, the reaction can be initiated using light to promote photo-excited holes. PSi may also be formed by stain etching when electrochemical etching is not possible. [16]

The exact nature of pore matrix is strongly dependent on the parameters used to form the structure, such as etching current density, substrate resistivity, doping type and crystal orientation. [17] On the optical scale, PSi thin films appears as a uniform thin film with well defined optical properties characterised by a mean field effective medium model.[18] In heavily doped silicon substrates the pores are etched preferentially in the <100> crystal plane leading to a strong asymmetry in the microstructure of the films, which leads to significant anisotropy in the refractive index. For substrates oriented in the <111> direction optical birefringence is observed at normal incidence.[19] As the porosity may be set, within certain constraints, to any value through the applied current, the refractive index may also be tuned over a large range of values, typically between 1.3 and 2.7.

The early demonstration by Berger *et al.* of creating monolithic optical superlattices out of multiple PSi layers with differing porosity provided a route to expand on the photonic capabilities of the material.[20] In quite the opposite sense to vacuum deposition, PSi multilayers are produced by etching new regions of PSi beneath the existing layers whilst still maintaining optical properties of the films. The porous films also form at a constant rate allowing the thickness of the films to be controlled by the etching time. Applying a series of current pulses, where the porosity and thickness of each layers is determined by the magnitude and the duration of the pulse, respectively, forms multilayered structures. High quality planar photonic structures with a variety of optical properties have been realised in this fashion and include, Bragg mirrors,[21] omni-directional reflectors, [22] microcavity resonators,[23] and graded index Rugate filters.[5] In the area of biosensing, resonant structures are able to provide improved sensitivity in the detection of low concentration of analytes.

The function of the optical sensing mechanism of the PSi films can best be understood in terms of interference from a single film of PSi. In such structures, reflectance interference fringes are observed in the visible and near infrared, and the fringe maxima are determined by the optical thickness of the film. The inclusion of materials, scuh as fluids and gases, within the intervening porous matrix will change the composition of the film leading to a change in the effective refractive index. This change in the effective refractive index alters the spectral positions of the fringes. Mesoporous silicon, with average pore dimensions ranging between 2 nm and 50 nm,[24] provides sufficient space for admitting large biological molecules into the matrix whilst still maintaining optical quality of the films.

Large compositional changes within the porous layers, such as the displacement of air in the voids with fluids, leads to dramatic shifts in optical properties, where large spectral shifts of the order of a hundred nanometres are observed. This has been used for on-off switching based sensors and indicators, where the colour of the sample changes markedly after a detection event.[25] Such changes have also been used for the detection of the ingress of different solvents and solvent vapours.[26]

Importantly, because the internal surface area of PSi occupies such a large volume of the film, it is possible to elicit a bulk refractive index response from surface interactions. Thus materials absorbed or desorbed from the internal surface can, in principle, yield substantial spectral shifts in films. This property distinguishes it greatly from other types of refractive index based sensor as the internal surface can be controlled to selectively bind analytes of a particular species whilst inhibiting general non-specific absorption, which would also contribute to spectral shifts in the optical properties. Read out methods typically focus on measuring changes in reflectance or transmittance, however other methods of read-out, such as luminescence, can also be used. [27]

The spectral shifts associated with binding or releasing events at the pore walls are typically small and difficult to observe in simple thin-film structures without some degree of data processing.[28] Resonant photonic structures provide a means of producing higher sensitivity and a less ambiguous response. (Figure 1) illustrates the observed shifts in the reflectance spectra for three typical structures; a single layer thin film, microcavity and Rugate filter. In the case of the single thin film, interference from the front and back dielectric interfaces leads typical oscillatory patterns in the reflectance spectrum where the pitch and magnitude is governed by the thickness and refractive index contrast respectively. In the case of the microcavity two dielectric mirrors provide highly reflecting interfaces which bound a cavity layer, leading to Fabry-Perot oscillations within the cavity. For the Rugate filter, the corrugated refractive index profile provides coherent reflections across bulk of the film leading to a sharp narrow peak in reflectivity, where the width and height of the peak are dictated by the refractive index contrast and number of periods.

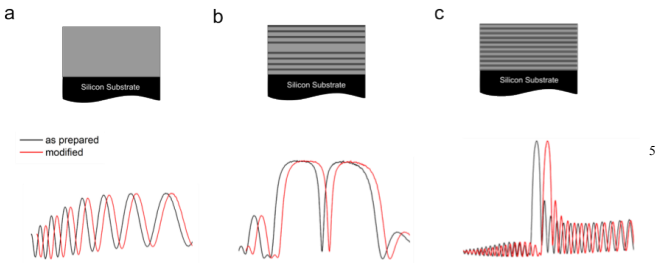

Figure 1. (top) Schematic diagram depicting structural cross-section and (bottom) observed shifts in the reflectance spectrum for three typical PSi photonic structures used in sensing applications; (a) single layer, (b) microcavity and (c) Rugate filter. The single layer is uniform thin film of several micrometres and produces multiple interference fringes in the visible and near infrared spectral regions. The microcavity is based on a Fabry-Perot resonator with two dielectric mirrors surrounding a cavity layer. The mirrors or composed of alternating layers of high and low porosity PSi of quarter wavelength thickness. The resulting reflectivity spectrum has a characteristic broadband high reflectivity band with a dip in the centre corresponding to the resonant cavity mode. Rugate filters consist of films with a sinusoidal refractive index modulation; when the refractive index variation is small a sharp peak is observed above the background of the thin film interference fringes. This type of spectral feature can equally be achieved using Bragg reflectors with a small refractive index between the layers. In all cases a redshift in the spectral features is observed when a material is deposited on the internal wall of the mesoporous scaffold and is the type of shift associated with an affinity based biorecognition interface. The advantage of using a more complex photonic structures is that the cavity resonance (b) and high reflectivity band (c) can be significantly narrower then the equivalent thin films interference fringes and is clearly observed above other spectral features.

When an organic analyte (n ~ 1.4) binds to the internal pore walls the effective refractive the PSi film increases as a fraction of the fluid (n = 1.33) or air (n = 1.0) is excluded from the pore. In all of the structures, the spectral features shift to the red indicating that the optical path in the films has effectively increased. Whilst the magnitude of spectral shift per refractive index change is similar in all of these structures, the change in the reflectance at a fixed wavelength, as a function of the refractive index change, is greatly enhanced. In the case of microcavity structures the line-width of the resonance can be as small is 0.2 nm at 1550 nm, whilst reflectivity bands for Rugate peaks are typically 10-20 nm. As typical spectral shifts observed in an optical biosensor are on the nanometre to sub-nanometre range, the need for resonant features is crucial for measuring binding events at the low detection limit.

The use of highly resonant photonic structures, such as microcavities, improves the capacity of PSi for spectral sensitivity; however, the corresponding introduction of regions of small pores in the low porosity region has the disadvantage of inhibiting target molecules from reaching the sensing surface. For example, the use of high refractive index, low porosity layers within the mirror region of the microcavity exclude large macromolecules from the cavity layer where optical mode is most sensitive to refractive index changes. This then raises the detection limit and leads to prohibitively long incubation times - it also excludes the possibility of doing reaction kinetics type measurements. Work by Delouise and colleagues tried to reconcile the issue of mass transport in high quality microcavity biosensors by increasing the average pore sizes in all layers to admit biomolecules through post processing.[29] Using such a strategy pore enlargement up to 50 nm was achieved with only a small reduction in optical quality. Attempts to extend the microcavity structures to macoporous did impact substantially on the optical resonance[30]. The best compromise for multi-layered structures appears to be the Rugate filters, or narrow band Bragg reflectors, where the refractive modulation is small, providing minimal disturbance to the diffusion of target molecules and whilst providing sharp spectral features for improved spectral sensitivity.

2.1 Alternative photonic architectures

PSi optical waveguides and other in-plane light confining structures, have certain advantages over planar structures in terms of coupling optical modes with sensing interfaces. For example, waveguide modes may be located close to a fluid interface that is accessible to large macromolecules and changes in the refractive index of guiding layers can be used to control the coupling wavelength through a prism or grating coupler, thereby providing an alternative optical transducer mechanism.[31,32] A number of waveguide architectures have been implemented using PSi as the core and cladding material, including planar, buried & ridge waveguides. Wave-guiding structures may be fabrication using lithography or by direct laser writing. [33] In general the optical loss present in these waveguides are quite large owing to the porous microstructure of the films and surface roughness at the core / cladding interface. [34] These factors are significant when measured over macroscopic propagation distances. One route to improving the waveguiding properties of PSi is to oxidise the silicon which reduces the refractive index contrast between the pores and voids, [35] however this restricts the use of robust hydrosilylation chemistry for surface functionalization, as will be discussed. Another novel sensing mechanism available in the waveguide geometry is to control the propagation losses through the inclusion of solvents in the pores; when the optical losses drop there is increase in the intensity at the exit facet. [36]

Another approach is to use microfabricated diffraction gratings where the grating period is influenced by the bulk change in refractive index of the PSi.[37,38] This particular geometry is self-referenced when comparing diffracted orders with the diffracted orders and again enables open access for molecules to penetrate into the film. Another unique feature of this approach is that the read-out mechanism is done via imaging rather then spectroscopy, which can be advantageous in some situations. Fabrication of in-plane periodic structures may be achieved post-fabrication using novel lithographic techniques, such as nano-imprint lithography. Similar in plane structures may also be achieved using light patterning during the etching of n-type PSi films. [39]

The introduction of new optical geometries such as Bloch surface wave modes may offer a good compromise in achieving high spectral sensitivity and with optimal location of the sensing surface.[40] Analogous to surface plasmon polaritons modes in metallic films, Bloch surface waves form at the interface between a uniform dielectric material and a photonic band gap material, such as a Bragg reflector and has an exponentially decaying profile in both regions. Bloch surface waves may be excited by resonant coupling techniques (e.g. attenuated total reflection) and as the mode volume of the Bloch surface wave is concentrated at the interface there is almost optimal overlap between the sensing volume and the target molecules to the sensing region. Further, by structuring the films in the lateral dimensions additional sensitivity may be gained by engineering the dispersion properties of the modes to provide a greater shift per refractive index change.[41] Bloch surface waves sensors have been recently implemented in the detection of protease activity[42] and as well as in gas sensing.[43]

2.2 New hybrid structures

Many of the early sensing devices made exclusive use of the intrinsic properties of PSi – pore infiltration, luminescence, thin-film interference and the adsorbing properties of native oxides. However, not all of these properties are ideally suited to sensing applications. For example, strong luminescence in PSi, which is a favourable as a read-out mechanism, suffers from quenching and is coupled with very small pores, which exclude large macromolecules, and readily oxidised surfaces.[17] Surface functionalization provided the first steps towards independent optimisation of sensing elements and resulted in marked improvements of specificity in detection. Incorporating PSi with other functional materials into hybrid arrangements enables the possibility of creating truly optimised optical sensing transducers with a more diverse range of properties.

The possibilities for hybridisation are possible through a number of different schemes. Using the nanostructured scaffold as a host for supporting nanoscale objects that provide additional functionality to the photonic structures, e.g. luminescent colloidal quantum dots[44] or magnetic nanoparticles. Freestanding PSi films can be transferred to different supporting substrates that are more suitable for particular applications (e.g. transparent, biocompatible, and/or flexible substrates). Even disparate materials can be combined with PSi into hybrid multilayered photonic structures using appropriate assembly techniques[45]. This flexibility in hybridisation opens the door to many opportunities for new biorecognition interfaces, photonic architectures and detections schemes as well as additional functionality such as self-assembly,[46] micromanipulation, and drug delivery.

The high sensitivity required for measuring trace quantities of molecules, also comes with a need for selectivity in detection and stability against long-term drift of the spectral properties, whatever the photonic structure or optical measurement technique used. Refractive index changes in highly porous materials can be the result of many factors and there are very few cues that can be used to delineate individual processes. Generally, resonant photonic structures indiscriminately provide higher sensitivity to all process that yield optical shifts and in the presence of competing processes have limited capacity improve the effectiveness of the optical biosensor. Thus, appropriate surface chemistry is needed to stabilize surfaces against oxidation, inhibit non-specific binding events, in addition to providing the appropriate receptors for target analytes.

3. Fabricating the Biorecognition Interface

The, as produced PSi, presents hydrogen terminated silicon species at the pore walls. Once exposed to air or water the exposed silicon hydrides (Si-H_x, x = 1, 2 or 3) is prone to oxidation to silicon dioxide among other oxide species (Figure 2). It is these silicon oxide species that give PSi its purported biocompatibility as in water they corrode releasing orthosilicic acid species which is the natural form of silicon found in the body.[3] This incredible advantage of PSi for *in vivo* applications is also a major drawback for biosensing and optical applications. This is because the refractive index of silicon oxides is around 1.4 while that of silicon is 3.5, and hence there will be a blue shift in the optical signature of the PSi when it corrodes. This means the corrosion reaction will lead to signal drift. The signal drift will continue until the PSi corrodes away completely.[47, 48] Further, the degradation of the material also means that any surface chemistry designed to give the PSi photonic crystals specificity for a given analyte can also be lost. Thus stabilising the PSi in aqueous solution and biological fluids over the timescale of the measurement has been an enduring challenge in using PSi in biosensing.[13] The solution to this challenge lies in surface chemistry that stabilises the PSi against dissolution.

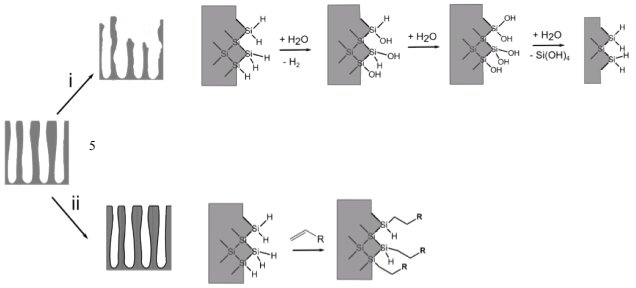

Figure 2 (i) Depiction of PSi oxidation and corrosion in solutions. (ii) Modification of PSi with organic monolayer *via* hydrosilylation of alkenes with hydride-terminated PSi to render the surface inert.

Although many different strategies have been developed to modify PSi for biosensing applications, including simply oxidising the surface, using polymers or simply adsorption of biomolecules, the vast majority of studies use either reacting the oxidised silicon oxide surface with organosilicon compounds[46] or reacting the hydrogen terminated silicon with alkenes or alkynes (Figure 2).[8, 13]Alkyl silane chemistry essentially involves oxidising the surface and then stabilising this oxide with a close packed monolayer that limits the accessibility of water to the underlying silicon oxide surface. Reactive groups at the distal end of the monolayer then allow further modification of the surface with biomolecules. This is the surface chemistry that was used in the seminal Lin *et al.* paper[4] where small molecules and DNA were immobilised. Since then, the same class of surface chemistry has been used for the immobilisation of small molecules,[49] DNA,[27, 50, 51] antibodies[52-54] and enzymes.[55-59] However, these early surface modification studies using this surface chemistry showed that it was prone to forming multilayers and was insufficiently stable for long term application in aqueous media[51], again because of the Si-O bond that forms being prone to hydrolysis[46] as is the case in oxidised nanostructured silicon. Hence a more stable surface chemistry is required.

The discovery that hydrogen terminated silicon surfaces could be modified by alkenes and alkynes by Linford and Chidsey in 1993[60, 61] provided this more stable surface chemistry. Alkyl chains with a terminal alkene or alkyne react with the Si-H species to give a highly stable Si-C bond (Figure 2) that is not subject to hydrolysis or multilayering.[7, 8] Many different strategies have been explored to cause this hydrosilylation reaction to happen but thermal hydrosilylation and UV induced hydrosilylation are the most popular and successful strategies employed[8]. Some examples of Si-C linked biorecognition interfaces formed by hydrosilylation include: DNA,[62] enzymes,[57, 58] small molecules,[63-65] hybrid lipid bilayer membranes,[66] antibodies, and cells.[67] It is to the application of this type of surface chemistry to forming biorecognition interfaces that we have made our own major contributions to PSi based biosensing.

It is worth considering what this surface chemistry is required to achieve and the strategies we have taken to fulfil these tasks. For PSi devices to effectively transduce a biorecognition event the following criteria must be met: 1) the PSi must not degrade such that a stable optical signal is obtained if no biorecognition event occurs, 2) non-specific interactions with interfering species in a complex biological sample must be prevented, 3) a surface must be selective for the analyte which typically requires a recognition moiety to be attached to the surface and 4) in some cases, such as using PSi biosensors in cell biology, different surface chemistry must be provided to the exterior of the PSi relative to the interior pore walls. Hydrosilylation of ω-functionalized alkenes on PSi is a convenient route to fulfil all these requirements.

In our work we initially attempted to get the one molecule to fulfil the first three criteria in a single modification steps. This molecules were designed that had a 10 or more carbon alkyl chain to provide a close packed monolayer to protect the silicon against oxidation, oligo(ethylene oxide) moieties to limit nonspecific adsorption of proteins and cells and epoxide[68] or hydroxyl[69] moieties on the distal end of the monolayer forming molecules to allow further coupling of biomolecules. However, such a strategy failed to provide effective passivation of the silicon surface which continued to degrade in aqueous media.[47] The solution to this problem was to fabricate the interface in a stepwise manner,[46] with the different chemical functionalities attached to the interface one component after the next.

The initial strategy employed to fabricate a stable biosensing interface in a stepwise manner was to first attach undecenoic acid or 10-succinimidylundecenoate to the Si-H terminated PSi surface to form a close packed monolayer that protected the PSi from the ingress of water and hence oxidation (Figure 3i). Subsequently, an oligo(ethylene oxide) species was attached to the surface bound carboxylic acid to provide resistance to nonspecific adsorption. Finally, protein or other biorecognition species could be attached to the end of hydroxyl terminated oligo(ethylene oxide) species.[47, 64, 70] Using this strategy, the quality of the initial base layer could be varied to determine the time over which the PSi photonic crystals would be stable in biological media[70] with the maximum time achieved before the PSi completely dissolved reaching up to 60 days.[47] Furthermore, by forming the base layer using 10-succinimidylundecenoate, water could be excluded from entering the pore spaces such that the exterior surface could be modified with one biorecognition species and the interior of the photonic crystal with a second species.[67] In this way PSi biosensors could be fabricated that allowed cells to be captures on the outside of the devices and material released by the monitored as they entered inside the pores.[13, 67]

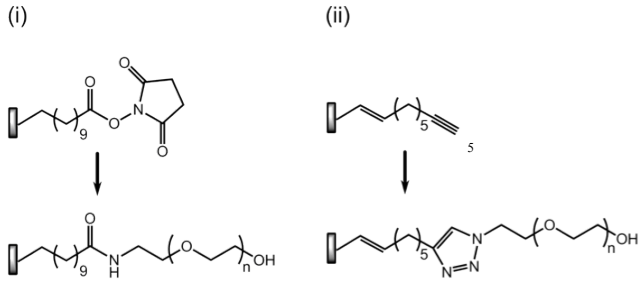

Figure 3 Chemical strategies for modifying PSi with monolayers to stabilise the material against oxidation and corrosion close-packed monolayers. (i). In the first approach the hydride terminated PSi surface is modified with 10-succinimidylundecenoate to form a close packed monolayer. Subsequently, an oligo(ethylene oxide) species is attached to the 10-succinimidylundecenoate species. (ii). In the second strategy the PSi surface is first passivated with a dialkyne *via* hydrosilylation. Subsequently, an oligo(ethylene glycol) layer is linked to the alkyne *via* click chemistry. Various coupling schemes are available to link the desired biomolecule to the reactive groups at the surface of the oligo(ethylene glycol) layer.

More recently the base layer has been fabricated using the dialkyne 1,3-nonadiyne which covalently couples to the surface via one alkyne and the distal alkyne is amenable to further reaction via the most well known click reaction, the copper assisted azide-alkyne cycloaddition (CuAAC) reaction (Figure 3ii).[65, 71] Thereafter, the rest of the surface chemistry is the same. The reason for changing to the dialkyne is that this base layer has been shown to react more rapidly and with higher density than with alkenes. The result is a base monolayer that protects the underlying silicon from oxidation more easily and with far greater effectiveness. The absence or presence of a ligand to protect the copper catalyst provides control over whether species are attached on the exterior surface or the interior pore walls. Furthermore, the click reaction to couple further species to the surface, is much more controlled that the amide bond formation used with the 10-succinimidylundecenoate.

In summary, these surface chemistry developments provide the opportunity to form truly stable PSi biosensors for use in cell biology and potentially *in vivo*. They can be applied to PSi particle[12] as well as macroscale PSi chips.

4. PSi based Biosensors

Resonant photonic structures coupled with highly functional surface chemistry provides a flexible platform for detecting a variety of different biomolecules, and opens opportunities to study a range of different biological systems under physiological conditions. In this section, different strategies for biomolecule immobilisation and application in biosensing are reviewed with an emphasis on some key developments rather than an exhaustive overview.

The very first PSi biosensing paper by Lin *et al*.[4] demonstrated that PSi could be used as a transducer and be integrated with a number of biological species including small molecules such as biotin, the steroid digoxigenin, short DNA oligonucleotides and proteins (streptavidin and antibodies). In that work, a simple single layer thin-film interference was employed. The PSi was oxidised to allow silane chemistry to be used for the attachment of biomolecules. This work by Lin *et al.* highlighted the possibilities of attachment of variety of different types of biological molecules via different surface functionalisation methods. Following on from Lin *et al*, Ouyang *et al*. used a more sophisticated PSi photonic device, a microcavity to demonstrate immobilisation of small biotin biomolecules to detect the capture of streptavidin. There was a wavelength shift toward longer wavelengths (red shift) in the reflectance spectrum of the microcavity and this shift increased as the biotin concentration increased. The biotin coverage inside the pores was estimated to be 95%, which was linearly related to the observed red shift. After exposure to streptavidin, a further red shift was detected which was attributed to the specific binding of streptavidin to the biotin-derivatised macroporous microcavity. On the basis of this effect, Ouyang *et al.* demonstrated a label-free assay of protein affinity to a biotin functionalised PSi surface.

Continuing the trend of immobilising small molecules recognition species to the PSi surface, Chan and co-workers[72] functionalised a synthetic organic receptor molecule, tetratryptophan *ter*-cyclo pentane (TWTCP) that specifically binds to diphosphoryl lipid A in water. Lipid A is highly conserved among different classes of lipopolysaccharides (LPS). LPS is a primary constituent of the outer cellular membrane of Gram-negative bacteria, therefore by selectively modifying the PSi with a specific receptor molecule, it was shown that Gram-negative bacteria could be detected based on the principles of light interference across multi-layers of varying refractive indices of a PSi microcavity resonator. In this work, they utilised the photoluminescence properties of the microcavity to recognise the binding event of the TWTCP receptor with the lipid A present in the bacterial cell wall along with the high surface to volume ratio of PSi to immobilise the receptor molecule.

Beyond small organic molecules as ligands, to immobilising biological molecules, further work by Chan and co-workers[27] functionalised

a PSi microcavity resonator for the detection of larger molecules, viral DNA. Lambda is a double-stranded DNA bacteriophage of *Escherichia coli, which is* a full-length viral DNA molecule. It was detected with this microcavity resonator biosensor by immobilising a complementary strand of DNA to PSi after silanisation of the surface. A red shift in the photoluminescence peaks was observed due to a refractive index change after the hybridisation of the two DNA strands.

Affinity-based interactions were also the subject of a study by Starodub and co-workers[73] who showed that mouse monoclonal antibodies induce little change in the photoluminescence intensity when physisorbed onto PSi. However, on binding to myoglobin, large changes in the percentage intensity of the photoluminescence were observed over a concentration range of 0.001-10 μg/mL in buffer solution. To demonstrate the effectiveness of the biosensor, the concentration of myoglobin (ng/mL) in human serum of patients suffering from heart failure was compared to ELISA test: the results showed that the data obtained from both methods correlated and their difference was no more than 5%. The overall time required for the analysis by the sensor was reported to be 15 minutes, which was considerably shorter than the time taken (no less than 3 hours) to complete the ELISA test. Following the trend of attaching antibodies to the PSi surface, Bonanno *et al.*[74] reported the fabrication of a label-free optical sensor for the detection of rabbit IgG in a more complex biological sample, whole blood, using a PSi microcavity. By leveraging size-exclusion filtering capabilities, the device was able to detect antibodies via a wavelength shift. Biotin-streptavidin chemistry was used to immobilise the antibody on the PSi surface. High target binding specificity, minimal cross-reactivity and a linear detection range of 2–10 mg/mL was established (Figure 4).

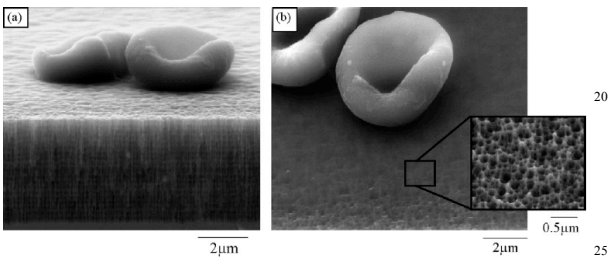

Figure 4 SEM images (a. Cross sectional view, b. Top view) showing the size-exclusion property of the PSi biosensor. Erythrocytes filtered out onto the PSi matrix and cross linked to the surface by glutaraldehyde fixation.[74] (Reproduced with permission from Ref. 74. Copyright (2007) Elsevier).

To demonstrate the potential of PSi based affinity sensors to be used in clinical applications, in another study, DeLouise *et al.*[75] reported the detection of opiates in a clinical sample of urine. Since the work involved the use of complex biological fluid, the surface chemistry employed in this work was more robust to oxidation and more complicated. This work was a progression on their earlier work where a competitive-inhibition immunoassay was developed in a PSi Bragg mirror to achieve improved detection of small molecule targets with a detection sensitivity range of 18 nM to 10.8 μM.[76] In this work, they used 3-ß-D-glucuronide, urinary metabolite of morphone/codeine, as an opiate analogue. It was covalently attached to a BSA-blocked PSi surface which had been aminosilanised using 3-(aminopropyl)tri-ethoxysilane. The test urine specimen was then added to the sensor chip directly followed by the addition of a fixed amount of antibody. Target opiate analyte in the test specimen competed with the surface attached opiate analogue for binding sites on the antibody. The amount of antibody bound to the immobilised opiate analogue is proportional to the target opiate analyte concentration. There was a characteristic red shift observed in the reflectance of these PSi Bragg mirrors once the binding event of the antibody to the opiate analogue took place. This study validates the analytical screening capability of label-free PSi biosensors and is the first quantitative demonstration of PSi biosensor technology for clinical use. Because the optical response from a PSi sensor can be specifically monitored to report binding events that occur within the porous matrix, the ability to filter a complex biological sample like blood provides an advantage over planar biosensing techniques. In addition, it has the potential for reducing cost and complexity of analytical techniques that rely on signal generation from secondary enzymatic or fluorescent molecules.

Another class of biological molecule that has been immobilised on a variety of solid surfaces like derivatised glass and silicon wafers is enzymes. The sensitivity of planar devices may, however, be limited by the maximum concentration of functional enzyme that can be incorporated within the designated area of the device. The use of PSi is a promising method to immobilise proteins and enhance the sensitivity of silicon based supports due to the large surface area of the pores in the structure, and the ability to fabricate a wide range of pore morphologies, which provides the PSi with the capacity to immobilise large amounts of enzyme. DeLouise and co-workers[77,78] have demonstrated this ability of PSi by immobilising a class of enzymes called Gluthione-S-transferases. In this work they oxidised the PSi microcavity thermally to enhance the enzyme stability in buffer solutions and create hydrophilic pore channels. This work showed that PSi could be used to quantitatively immobilise functionally stable proteins. This is of importance in achieving high sensitivity and sustained operating efficiency of a biosensor.

In contrast to using immobilised enzymes to detect the concentration of an analyte, there has been a recent shift in biosensors to switching the paradigm around and using immobilised enzyme substrates for the detection of the activity of enzymes. This strategy is particularly suited to PSi where the high surface area allows a large amount of substrate to be immobilised and the natural catalytic function of the

enzymes effectively provides an amplification scheme where a large amount of substrate can be degraded by a single enzyme molecule. It is also very important with regards to using PSi optofluidic devices for cell chips and for monitoring biological activity as will be discussed below. Recently PSi rugate filters have been used to monitor the activity of protease enzymes in particular[79, 80]. For example Orosco *et al.*[80] fabricated a PSi rugate filter that was made hydrophobic in the interior by methylation of the micropores. The hydrophobic pores then restricted the entry of large biomolecules and buffer solutions. The hydrophobic protein zein was adsorbed onto the top surface of the porous film, and the underlying pores remained air-filled. Incubation with proteases, in this instance with pepsin, led to zein digestion and subsequent infiltration of the small peptide fragments and water into the vacant pores. The pore loading caused an increase in the refractive index of the PSi layer, which, in turn, induced a measurable red shift to the reflectance band. With this biosensor, protease concentrations as low as 7 μM could be detected. Furthermore, with protease concentrations higher than 14 μM the changes to the porous matrix were so profound that they could be observed by naked eye. This work shows that PSi in conjunction with its ability to operate with natural enzymatic substrates can provide for a simple protease-activity assay, which can detect nanogram quantities of protease at room temperature (Figure 5).

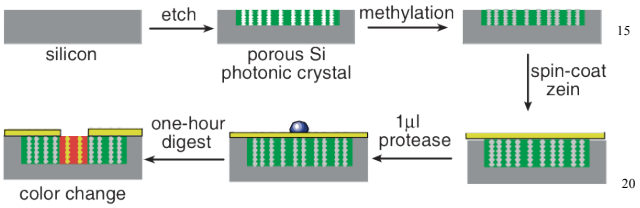

Figure 5 A schematic showing enzymatic assay using a protein-coated porous Si photonic crystal. A hydrophobic, photonic crystal is prepared by electrochemical etching of Si, followed by electrochemical grafting of methyl species to the inner pore walls. A thin layer of the protein zein is then added. The assay is carried out by addition of a small drop of solution containing active protease (pepsin), which digests the protein layer. Infiltration of proteolytic cleavage products to the photonic crystal leads to a color change that is readily observable to the naked eye.[80](Reproduced from Ref .80 with permission from The Royal Society of Chemistry).

Building onto this work further, Orosco *et al.*[81] reported a mesoporous silicon double-layer nanostructure, which comprised of an upper layer with pore diameter 100 nm and a lower layer with a pore diameter of 6 nm. The upper layer was able to capture the protease pepsin, host a catalytic reaction was able to occur in the mesoporous cavity once the substrate a-casein was added to the structure. Infiltration of the digested fragments into the lower layer produced a measurable change in optical reflectivity, and this allowed for label-free quantification of enzyme kinetics in real time within a volume of 5 nL. This work provided a general method to quantify kinetics of an immobilised enzymatic reaction as the device was able to monitor protein digestion in real time. Such a capability may be of interest to high-throughput analytical and synthetic communities, such as DNA amplification, polymerisation, enzyme-linked assays and protein purification.

Both the studies by Orosco *et al* together exploited the same basic principle of degradation of proteins by protease enzymes causes material to enter the pore spaces of the PSi and cause a discernable optical shift. An alternative method of protease detection involves the covalent immobilisation of the enzyme substrate within the mesopores of PSi such that the protease enzymes diffuse into the pores and degrade the substrate. Kilian *et al.*[82] immobilised a peptide in the pore of PSi to achieve this. The hydrogen-terminated silicon surface was first modified with the alkene 10-succinimidyl undecenoate via hydrosilylation. The monolayer with the succinimide ester moiety at the distal end served the dual function of protecting the underlying silicon from oxidation as well as providing a surface suitable for subsequent derivatization with amines. The surface was further modified with 1-aminohexa(ethylene glycol) (EG6) to resist nonspecific adsorption of proteins common in complex biological samples. The distal hydroxyl of the EG6 was activated using the coupling reagent disuccinimidyl carbonate for selective immobilization of peptides as protease recognition elements. Kilian *et al.*[82] exposed the peptide-modified photonic crystal to the protease subtilisin, which resulted in peptide cleavage. The generated amino acid fragments were removed from the porous layer, thereby reducing its refractive index. When the reflectance spectrum was measured in air, a blue shift of the photonic resonance was observed owing to the decrease of the refractive index. In comparison with the biosensor reported by Orosco *et al.,*[80] this device was able to detect considerably lower protease concentrations of 37 nM. More importantly, the work also provided for a PSi based biomaterial, which could be modified with different surface chemistries. Different surface functionalisations would allow for attaching peptides or biological sequences that could act, as a substrate for proteases or different enzymes likes caspases for example.

The examples above of PSi chip for the detection of protease enzyme activity are important as there exists a need for rapid assays of protease activity, since current schemes to quantify protease activity involve either fluorescent[83, 84] or colorimetric assays.[85, 86] These assays are time consuming and require relatively large quantities of enzyme. Proteases are required because of their pivotal role in intra-[87-89] and intercellular[90, 91] processes and is a major class of enzymes released by the cell to remodel their environment. Therefore studying their activity using PSi presents the possibility of detecting activity from cells for which PSi should be cell friendly. Specifically, the ability of this PSi material to detect chemicals,[92, 93] biomolecules,[94, 95] enzymatic activity[96] presents the possibility that PSi may play a role in *in vitro*

sensing or *in vivo* diagnostic devices in which the material is in direct contact with live cells.

To check whether surface chemistry affected cell adhesion and stability of the cells, another study was conducted where primary rat hepatocyte cells were cultured on PSi and their viability was determined by measuring protein production from the cells.[97] Here, the PSi surface was modified by ozone oxidation and coated with collagen. Cellular morphology was observed on the two surfaces and the authors demonstrated that surface treatment promotes cell attachment, with more cells attaching to collagen-coated PSi in comparison to oxidised PSi. Work done by Voelcker *et al.*[98] demonstrated that collagen-coated and amino-silanised PSi promoted cell adhesion of human iris epithelium cells and rat pheochromacytoma (PC12) cells whereas cells attached poorly to ozone oxidised and polyethylene glycol silanised surfaces. These examples confirm the importance of surface chemistries on PSi in the adhesion of different types of cells on PSi. Extending this concept, Khung *et al*. illustrated that pore size, in addition to the surface chemistry, is a significant variable in determining the cell adhesion capability. Human neuroblastoma cells prefer the large (1-3 μm) to small (100-300 nm) pores by comparison.[99]

With the demonstration that mammalian cells can thrive when cultured onto PSi surfaces, the combining of cells on PSi with biosensing to determine information about the activity or status of cells was a logical step in the development of PSi biosensors. Schwartz *et al.*[100, 101] have developed the concept of a so-called 'smart Petri dish', which enables monitoring of the health of cell cultures by means of light scattering from the surface of a rugate filter. The surface of a PSi rugate filter is illuminated with white light at an oblique angle, and a charge-coupled device (CCD) spectrometer was positioned perpendicular to the surface. Specular reflectance from the photonic reflectance band cannot be observed in this configuration. However, introduction of a scattering centre on the rugate filter surface, such as a biological cell, resulted in the scattering of light emanating from the surface, which can be detected by the spectrometer. Changes in the morphology of the cells on the surface, typically indicative of a decrease in viability, then causes a change in the scattered light. This report is an important advance in using PSi for cell biosensing and in cell chips, although biochemical information was lacking.

Biochemical information from cells adhered to PSi surfaces as a consequence of change in the solution environment around cells has recently been demonstrated. The study by Gooding and co-workers[13] built on earlier work by the same group on detecting protease activity.[82] Macrophage cells were adhered to the exterior surface of the PSi rugate filter, using the surface chemistry developed by Kilian *et al.*[67] where cell adhesive peptides were attached to the exterior surface of the PSi to capture the cells but different protease sensitive chemistry was attached to the pore surfaces. The cell type used was a macrophage cell that release protease enzymes upon certain stimuli such as the presence of a biomarker from a foreign species. The protease enzymes targeted were matrix metalloprotease 2 (MMP-2) and MMP-9, which are both gelatinases. Hence the interior of the pores was filled with gelatin. Once the cells were stimulated with lipopolysaccharide (LPS), which is found of the exterior of all gram-negative bacteria, the immune defense function of the macrophage cells causes an upregulation of the release of MMP-2 and MMP-9 from the macrophage cells. These MMPs then diffuse into the pores of the PSi, degrade the gelatin and a blue shift in the optical signature of the rugate filters is observed (Figure 6). The observed signal came from less than 1500 cells. However, it was estimated that the technique only required one in 30 pores to have the gelatin degraded. Such a finding is striking as it suggests that, in principle the methodology could be used for single cell analysis. The very high sensitivity in the instance arises from a simple but important conceptual advance in using PSi as a biosensor. Unlike previous work using PSi as a biosensor, the entire pores are filled with the material to be degraded and hence higher sensitivities were achieved. There is a parallel with the Orosco *et al.* study with zein proteins as in that study, the amino acid digestion products enhance the sensor's response by facilitating solution infiltration into the hydrophobic layer, replacing air with water. Hence again the change recorded relates to not just the surface of the pore[102] but the entire pore space.

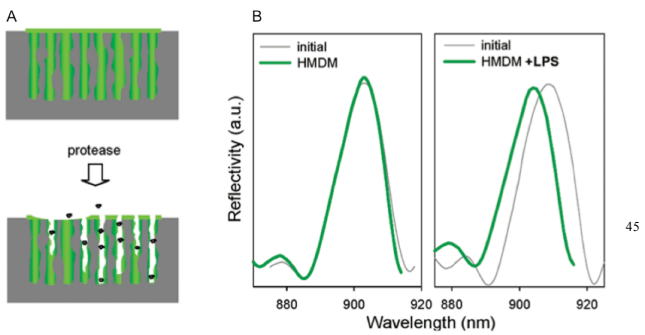

Figure 6 A. A schematic showing the degradation of gelatin inside the pores by the protease. The reflectivity shifts observed in the macrophage cells with the stimulation of cells with and without LPS.[13] (Reprinted with permission from Ref. 13. Copyright (2009) American Chemical Society).

5. Microfabrication of PSi for multiplexed optical assays

One of the requirements in biomedical research is to perform large number of analyses from small sample volumes.[103] This requirement has led to the development of multiplexing technologies. PSi is an ideal platform for label-free biosensing, and its applications in biological activity monitoring will be largely expanded by achieving multiplexed detection. This is particularly the case for using PSi in cell chips and cell based biosensors as recently demonstrated.[13]

To realise highly parallel PSi biosensors for multiplexed detection, it requires microfabrication to achieve microscale structuring of PSi.[103] The structuring and patterning that have been implemented by microfabrication fall into two main classes: microarrays and microparticles.[118] In addition, microfabrication can be applied to PSi so as to develop novel photonic crystal devices, which have the potential to be integrated with microfluidics to give optofluidics devices.[104]

This section will summarise recent studies that have been performed into the microfabrication of PSi, covering the fabrication processes and the related applications. The advantages and limitations related to the fabrication methods will be highlighted. Significantly, all fabrication methods mentioned here can be applied to other porous materials systems.

5.1 Methods of PSi microfabrication

Microfabrication of PSi can be achieved by combining well-established silicon microfabrication methods with PSi formation. Generally there are two broad strategies by which PSi can be locally patterned and/or miniaturized: i) by patterning a silicon wafer and then forming PSi such that the formation of PSi occurs in defined regions, or ii) by forming PSi first and then patterning such that selective PSi is modified or removed. For both two strategies, most of work has been performed using photolithography techniques, with a small proportion by other methods. The rest of the section will detail the two broad strategies respectively using photolithography methods first and then there will be a brief discussion of other methods.

5.1.1 Local anodisation of patterned crystalline silicon surfaces through a mask

The local anodisation employs photolithography to first form patterns of masking materials on crystalline silicon substrate, followed by performing anodisation through the masking layers to give spatially defined PSi. Photoresists are the immediate mask materials. The mask material is first deposited on the silicon surface, followed by photolithography to selectively remove some photoresist to give the pattern. Electrochemical etching is then conducted on the silicon surface covered by mask patterns. After anodisation, PSi in defined areas is produced (Figure 7). This method of local anodisation is highly desirable, because it is based on well-established microfabrication methods for flat silicon, and the patterned regions of PSi are well defined with the remaining area being crystalline silicon.

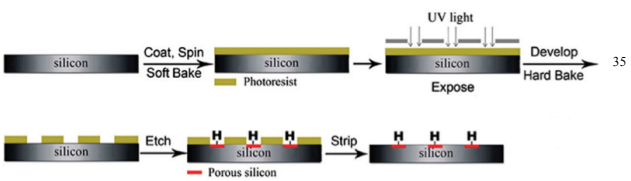

Figure 7 The procedure for local anodisation of crystalline silicon through patterned photoresist mask. The photoresist is patterned on silicon surface with desired features using the standard photolithography processes: the silicon substrate is first covered with photoresist by spin coating, and prebaked to drive off excess solvent from photoresist. The substrate is exposed to UV light through a photomask printed with the desired patterns. The exposure to light causes a chemical change to the photoresist that allows certain regions of the photoresist to be removed by a "developer" solution. The resulting substrate is then hard baked to solidify the patterned photoresist to make a more durable protecting layer for the subsequent PSi formation. Electrochemical etching is then performed on the patterned silicon surface to form localized PSi. For using other mask materials, additional deposition and fabrication processes are required before and after photolithgraphy.[105] (Reproduced from Ref .105 with permission from The Royal Society of Chemistry).

The method of local formation of PSi has been used to form discrete PSi areas on the microscale to fabricate microparticles and microarray chips for multiplex assays. For example, Chen *et al*.[105] prepared patterned PSi by local anodisation, followed by initiation of an atom transfer radical propagation polymerisation to grow (poly-ethylene glycol) methacrylate on the PSi regions. The substrate was subsequently used as a gel-pad protein microarray, and its function was demonstrated by a dynamic assay to explore the detection limit for an example system of NTA-Ni^{2+}/histidine-tagged protein with fluorescence measurement. In another example, Flavel *et al*.[106] fabricated micropatterned arrays of PSi, which were chemically functionalised with cell adhesion peptide to facilitate the selective attachment of human lens epithelial cells. The photoluminescent pattern of the PSi arrays was also found to be well-defined, which has potential applications as optical sensor arrays. In the aspect of microparticles, Cunin *et al*.[107] carried out local anodisation with photoresist patterned crystalline silicon to produced spectrum-encoded PSi particles. These multilayered PSi particles displayed a sharp peak in the optical reflectivity spectrum, and the coding information depended on the waveform used in the etching process. The encoding approach of the PSi particles was tested in an antibody-

based screening using both fluorescence and reflectivity information. . Ferrari and co-workers have conducted a series of work on PSi microparticles to achieve a precise control over the process of local anodisation of PSi, and produced finely tailored mono-disperse PSi microparticles.[108, 109] Their work into multistage drug-delivery system based on the PSi microparticles will be discussed in the following section.

It is noteworthy that, after local anodisation, the surface of the PSi region is terminated by silicon hydrides, while the surrounding non-etched flat silicon surface retains its native silicon oxide functionality. This difference in chemistry provides the potential for the PSi area to be further modified with chemical functionality while leaving the non-porous regions unaffected. This potential is particularly important for the selective immobilization of biomolecules for microarray application.[110] In the work mentioned above by Flavel *et al*.[98], the patterned PSi was modified by hydrosilylation with *N*-hydroxysuccinimide terminated alkene, and the *N*-hydroxysuccinimide ester was further covalently attached with functional molecules such as fluorescent dye or cell adhesion peptide (Figure 8).

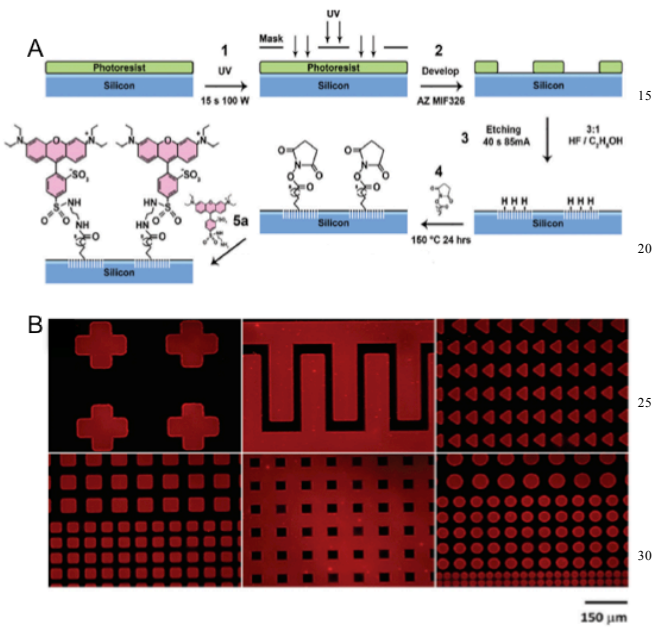

Figure 8 An example of selective surface modification for local anodized PSi surface. A. Schematic of local anodisation of PSi and the following immobilisation of lissamine dye on the PSi areas. After local anodisation, the surface of PSi patterns was hydride-terminated while the surrounding flat silicon that has not contacted with hydrofluoric acid retains its native silicon oxide functionality. The PSi regions were then modified by hydrosilylation with *N*-hydroxysuccinimide and attached with lissamine dye. B. Fluorescence microscopy images of patterned PSi after lissamine immobilization show a strong fluorescence contrast between the PSi arrays and the surrounding regions.[98] (Reprinted with permission from Ref. 98. Copyright (2011) American Chemical Society).

A variety of masking materials have been used for local anodisation of silicon surface, such as photoresist, silicon oxide, silicon nitride and cross-linked polymers.[109, 111-113] Photoresists are the most used masking materials, mainly because they form patterns immediately and can be removed easily by organic solvents. Although photoresists have been widely used as mask for local formation of PSi, they are only effective for short anodisation time or low current density. During anodisation of PSi, the attack of hydrofluoric acid and ethanol weakens the adhesion between the photoresist and silicon surface, and an anisotropic undercut takes place at the edge of the masked areas. The problem of the anisotropic undercutting largely limits the structure size and distance between PSi areas.[111, 112]

The strong anisotropic undercutting by photoresist can be reduced by using other mask materials. Silicon nitride by chemical vapour deposition is demonstrated as an effective masking material and it shows good resistance to hydrofluoric acid during PSi anodisation.[114] Mask removal of silicon nitride is not as simple as that of photoresist however. Nevertheless, the silicon nitride can be removed in concentrated hydrofluoric acid, a process compatible with PSi. Alternatively, the surface can be used as formed due to different physical and chemical properties of PSi and silicon nitride.[108, 109, 115]

Although local anodisation of PSi is used widely, there are potential drawbacks of this method. Firstly, apart from the anisotropic undercut introduced by mask layer with weak adhesion such as photoresist, another type of undercut takes place regardless of mask materials, which is known as isotropic undercutting. That is, the undercutting occurs equally in all directions. As a result of the isotropic nature of anodisation process, lateral etching occurs with an extension equal to the thickness of PSi layer depth.[112, 114] This isotropic undercutting limits the miniaturization of PSi pattern size, especially when there is a specific requirement for the thickness of PSi to achieve certain optical structure. In addition, because of the edge confinement from etching cell configuration and electrical field distribution in etching process, non-uniformity occurs between the edge and centre areas of PSi surface. After patterning the mask layers on silicon surface, each silicon

spot forms a small etching cell with edge confinement by the mask. After anodisation, the non-uniformity will occur in each individual PSi spot. The non-uniform optical properties due to edge effects is exacerbated when forming microdomains of PSi after patterning because the edges present a much larger portion of the material than macroscale porous silicon. Hence, if optical properties of each PSi spot are to be considered in sensing application the anisotropy is undesirable.[107, 116]

The undercutting problems associated with local anodisation through hard masks can be solved by maskless local formation of PSi. This is achieved by apply a localized surface modification to silicon surface before PSi formation that either promotes or inhibits PSi formation. The method to promote PSi formation can be achieved by metal-assisted chemical etching, which is an alternative method for PSi formation to the common electrochemical etching. In this method, a thin metal film is deposited on silicon surface and acts as catalyst that promotes the etching of PSi without the need of external bias. This concept provides a strategy for local formation of PSi by means of selectively depositing catalyst metal to silicon surface and then performed chemical etching.[110, 117, 118] Li *et al*.[102] prepared PSi protein microarrays by combining metal-assisted chemical etching and photolithography process. They compared this method with automatic spotting on a homogenous PSi surface, which is a commonly used method to produce protein microarrays, and found the former presented a homogenous microarray image with a clean background, while the spotted surface was disordered and had more non-specific adsorption on the background. This work indicates that the locally formed porous silicon patterning by photolithography technology is suitable for the application of PSi-based protein microarrays. In addition, local metal-assisted chemical etching was used to produce vertically aligned silicon nanowire patterns and nanoscale three dimensional PSi patterns.[117, 118] For the method of localized modification that inhibits PSi formation, microcontact printing, which is a soft lithographic technique capable of produce microscale monolayer patterns, was used to pattern passivating monolayers on silicon surface for mediating further PSi local formation. Harada *et al*.[110] fabricated PSi arrays by microcontact printing coupled with Pt-mediated etching. In their method, octadecyltrichlorosilane monolayers were firstly patterned on a Si substrate which served as a passivating pattern. A Pt(0) complex was then coated on the surface and only deposited in areas not covered with octadecyltrichlorosilane, which led to the local formation of PSi by metal-assisted chemical etching. This strategy produces an alternative approach for the time-consuming lithographic processes to direct the local formation of PSi.[116, 119]

The local formation of PSi can also be achieved without the use of any mask or pre-treatment through direct light-induced etching. By projecting lithographic images onto silicon wafer during anodisation, Doan *et al*.[120] fabricated patterns of luminescent PSi on silicon substrate with a lateral resolution of 20 μm. The patterning was achieved on both *n*-type silicon by photoanodic etching and *p*-type silicon by photocathodic protection.

5.1.2 Patterning uniform PSi films through microfabrication techniques

The problems of undercutting and edge effects associated with local anodisation of flat silicon jeopardize the optical properties of microstructured PSi. The variation in optical properties as a result of selective anodisation can be avoided by means of first forming the PSi structure, and then performing patterning using microfabrication techniques. This method has mostly been employed to achieve patterned chemical functionality on PSi for cell patterning[121, 122] PSi micromachining for new concepts in photonic crystal[41] or to produce uniform sized microparticles[123, 124]. For surface chemistry patterning on PSi, which has the potential application in cell patterning, a homogenous PSi surface with different chemical functionalities at discrete locations is more advantageous than a surface with different regions of PSi and flat silicon which is normally produced by local anodisation. This is because the former method completely excludes changes in the surface topography between porous structured surface and flat surface, which may influence cell behaviour.[122]

Photolithography remains the main technique involved in generating different chemical functionalities on PSi surface. After the PSi surface is covered with a lithographic mask, the first chemical functionality can be introduced to the exposed regions. The second functionality can be introduced subsequently after mask removal.[122] This strategy has been demonstrated using both the surface chemistries involving silanisation and hydrosilylation of alkenes. Sweetman *et al*.[115] demonstrated the ability to produce two different chemical functionalities to discretely patterned areas on a PSi surface using a combination of photolithography and silanisation. The whole PSi surface was introduced with the first functionality by the first salinization, followed by the patterning of photoresist on the surface by photolithography. The silane in the exposed regions was then removed, and the exposed region was reoxidized and subjected to the second salinization. After removing the photoresist, the PSi surface was presented with two different functionalities on defined regions.

Performing photolithography directly on a PSi surface is similar to the well-established processes for flat silicon, yet it has some unique challenges to which one needs to pay attention. First of all, it is known that if photoresist is applied to a porous layer it penetrates into the pores. The removal of the resist from the pores can be difficult and may impede further chemical modification of pores.[125] As a result, it is helpful to first cover the surface with a protection layer, usually deposited metal or silicon dioxide, to prevents resist from penetrating into the pores, as well as improving the surface homogeneity for subsequent resist spin-coating and photolithography.[126, 127] In addition, freshly prepared PSi is easily dissolved in alkaline solution, of which most of the positive photoresist developers are made. Although the problem can be avoided by using negative photoresist and related solvent based developer, it largely limits the range of applicable photoresists and complexes the lithographic process. This problem can be solved by surface stabilization methods such as annealing in nitrogen atmosphere or introducing closely packed monolayers that are resistant to alkaline conditions, or again using a protective layer on the surface to prevent underneath PSi from contacting with the developer.[125, 127]

Light-assisted hydrosilylation of alkene/alkyne species on PSi structure provide a strategy to directly pattern chemical functionalities on

PSi without lithographic hard mask.[128] In the important work by Sweetman *et al.*[121], the first alkene species with *N*-hydroxysuccinimide linker was attached on patterned PSi areas by irradiating the surface through a photomask via a hydrosilylation reaction, and a second alkene species with a polyethylene glycol functionality was attached to backfill the non-reacted surface sties by another hydrosilylation step. The surface was selective immobilized with cell adhesion mediator in *N*-hydroxysuccinimide-functional regions and then used for mediate cell patterning. (

Figure 9).

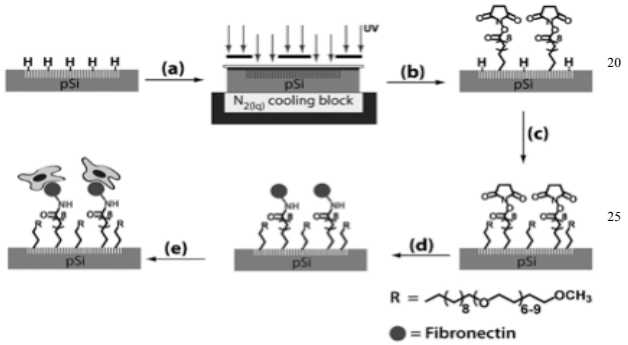

Figure 9 Chemical patterning strategy using light assisted hydrosilylation. The first alkene species is attached by UV initiated hydrosilylation, with the initiated regions defined by a lithographic photomask plate. The area that has not been reacted is then attached with the second alkene species by another hydrosilylation step. In this specific case, the PSi surface is first immobilized with N-hydroxysuccinimide ester alkene, which was further conjugated with fibronectin that has the ability to mediate cell adhesion to the surface. The surrounding areas were modified with polyethylene glycol alkene which prevents cell attachment. The chemically patterned PSi surface can be then used for mediate cell patterning.[121] (Reproduced with permission from Ref. 121. Copyright (2012) Wiley-VCH).

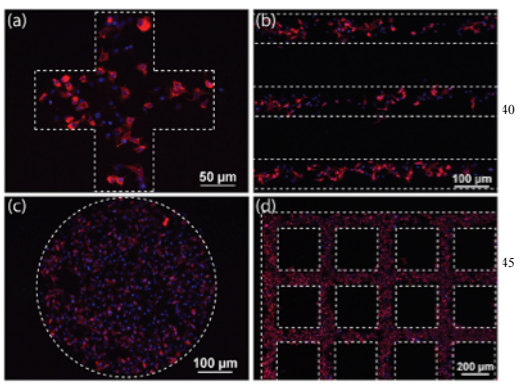

Figure 10 Fluorescence microscopy images of cell patterning on PSi. SK-N-SH human neuroblastoma cells were cultured on the functionalized PSi surface, and stained with Hoechst and phalloidin for observation. The surface for cell adhesion has been functionalized with fibronectin, while the non-cell adhesive area has been immobilized with poly(ethylene glycol) antifouling species. The images demonstrate the versatility of the surface patterning technique in terms of possible sizes and shapes of patterned features.[122] (Reproduced with permission from Ref. 122. Copyright (2012) Wiley-VCH).

The direct photopatterning method by light-assisted hydrosilylation avoids the issues associated with lithography on PSi, However, there is an incompatibility between the hydrosilylation conditions and standard lithography facilities. Hydrosilylation reaction must be performed in an inert atmosphere with completely deoxygenated and dried reagents to prevent the formation of silicon oxides during the monolayer formation[6] while lithography process is performed in clean room with an integrated mask aligner facility. Because of this incompatibility,

direct photopatterned hydrosilylation cannot be conducted in a clean-room where lithography is processed. The dusty laboratory condition limits the spatial resolution that photopatterned hydrosilylation can achieve compared to lithography patterning.

Besides light assisted hydrosilylation, there are other methods to introduce different chemistries on PSi surface by direct modification. Khung *et al*.[129] produced micropatterns of PSi films by direct laser writing. In their work, the whole surface of PSi was first functionalized with grafted poly(ethylene glycol) polymer to render the surface nonfouling ability and subsequently ablated with laser to form microscale patterns. Human neuroblastoma cells were found to selectively adhere on the laser-ablated regions of the micropatterns.

Chemical patterning of different functionalities on PSi surface has been widely used to mediate selective adhesion of cells.[121] By introducing cell-adhesive species on discretely patterned regions and antifouling layers on surrounding area, cells cultured on the surface will only adhere on defined regions. The patterning strategy is essential for cell-based multiplexed biosensors, cell culture analogues, tissue engineering, and fundamental studies of cell biology.[130] Voelcker and co-workers have performed considerable work on PSi micropatterning by microfabrication methods integrating with PSi surface chemistry strategies, and used the microfabricated PSi surface for selective attachment of mammalian cell (Figure 10).[122]

Apart from patterning different chemistral functionalities on a large PSi chip, in order to fabricate uniform-sized microparticles, there is a requirement to process PSi micromachining to form microscale structures. Ryckman *et al*.[131] developed a simple method of patterning PSi by direct imprinting. The desired patterns was firstly formed on a silicon stamp by standard lithography and reactive ion etching, and transferred to PSi surface by means of applying pressure to the pore structure to selectively destroy certain regions while leave others intact. The whole process was performed in a one minute and can be applied to other porous materials. In addition, the silicon stamp is reusable, which reduces the fabrication time considerably. Potential concerns with this approach are the possibility that the PSi inside the patterns might get damaged and the aspect ratio attainable by the direct imprinting is also limited.

Dry plasma-assisted etching is widely applied in silicon micromachining, mainly due to the achievement of etch directionality without utilizing the crystal orientation.[132] Integrating PSi with this technique will largely expand its application in fabrication of novel photonic crystal devices for biosensing. However, to date there are only a limited number of reports on PSi patterning for biosensing application using dry etching techniques.[41] This is because there are several challenges related to PSi dry etching. For example, the porous nanostructure makes the etching processes much more complicated than crystalline silicon, and it is even more challenging to maintain the required optical structure after reactive ion etching. In addition, the large internal surface of PSi renders the devices sensitive to contaminations such as polymer deposition during plasma etching, which is unfavourable for further surface chemistry modification. [120]

Even with the above challenges, successful attempts at employing dry etching of PSi for biosensing applications have been demonstrated. In general, after PSi film is formed, a hard mask of metal or ceramics is deposited on the PSi surface, which acts as a protective layer. Photoresist is subsequently patterned on the surface by lithographic process. The patterns are then transferred to PSi by reactive ion etching. Due to different etch rate between PSi and the mask material, the PSi regions exposed to the plasma are removed, while the areas under mask is protected (Figure 11).[133] PSi two-dimensional photonic crystal is formed after removing the mask material, and can be further fabricated into uniform-sized PSi microparticles by electrochemical lift-off and ultrasonication processes.

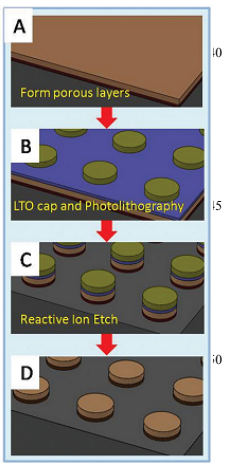

Figure 11 Process of patterning PSi by reactive ion etching combined with photolithography. In this particular case, after fabrication of PSi, a low temperature silicon oxide was deposited on the surface by a low pressure chemical vapour deposition. Photolithography was carried out on the surface to form photoresist patterning of circles arrays, which was then transferred into the silicon oxide and PSi film by reactive ion etching.[133] (Reproduced with permission from Ref. 133. Copyright (2012) John Wiley and Sons).

By adjusting the experimental parameters in reactive ion etching, PSi profile with vertical sidewalls has been produced for biosensing applications. Jamois *et al*.[42, 126] developed a PSi based surface-wave biosensor via reactive-ion-etching patterning to form two-dimensional PSi multilayer structure. The surface was then functionalized by silane chemistry and immobilised with DNA probes. The performance study demonstrated an increase in sensitivity by a factor 10 compared with one-dimensional PSi sensor without patterning (Figure 12). Meade *et al*. fabricated uniform sized PSi microparticles using chlorine-based reactive ion etching (Figure 12**)**, and employed the photonic crystal particles in a multiplexed DNA screening, which will be discussed in the following section.[124, 134] Note that microfabricated PSi microscale pillars with vertical walls via reactive ion etching are ideal for making uniform PSi microparticles.

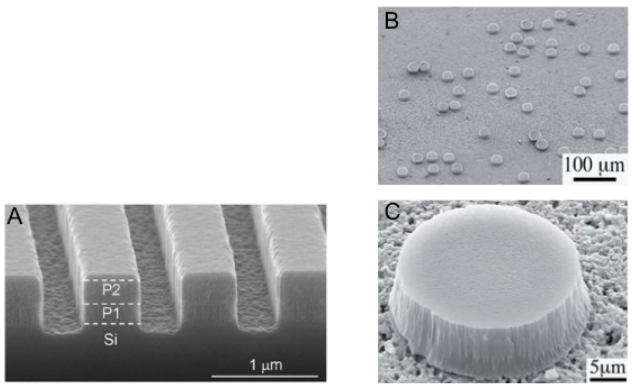

Figure 12 Scanning electron microscopy images of PSi micropatterned structures by reactive ion etching. (left) PSi two-dimensional photonic crystal shows PSi microscale trenches with air slits, (right) Scanning electron microscope images of uniform-sized PSi microparticles which reveal a monodisperse population.[34,116,126] (Figure 12b and 12c reproduced with permission from Ref. 116. Copyright (2007) John Wiley) and Sons.

6. PSi microparticles

The potential for nanomaterials as biosensors for *in vivo* applications has provoked great interests in nanoscale materials, such as nanoparticles, nanotubes and nanowires.[110, 135-139] Microfabrication enables the fabrication of uniform micrometer-scale and smaller PSi particles, which offers a number of interesting properties for cell-based biosensing applications. The unique optical features allow PSi photonic crystal particles to be easily identified and to perform label-free sensing by showing distinct reflectivity spectra in visible and near infrared (NIR). The NIR range is particularly attractive for *in vivo* applications because of the ability of NIR radiation to penetrate biological tissue. The convenient surface modification methods prepare PSi particles with flexibility in various sensing scenarios. More importantly, the low toxicity of PSi particles in biological environments creates an attractive alternative to other nanoscale materials for various cellular applications.

6.1 Biocompatibility

The main advantage of PSi in an *in vivo* biosensing system over many other biomaterials is its biocompatibility. In 1990s, Canham raised the possibility of using microporous silicon films as active biomaterials, by demonstrating *in vitro* that microporous silicon films could induce hydroxyapatite growth.[140, 141] Steinhauer *et al.* extended research into the biocompatibility of PSi by examining several biocompatible solid supports for preparing protein microarrays.[142] The results based on array spot morphology, protein signal intensity, sensitivity, signal to noise ratio and reproducibility, showed that macroporous silicon substrates were of high biocompatibility for protein microarrays.[142] PSi was also demonstrated to be an excellent biomaterial for cell culturing.[143-146] For example, the compatibility of primary rat hepatocytes was studied on an oxidized nanoporous silicon substrate, where cell viability and function remained for over two weeks.[147] Similarly, epithelial cells, endothelial cells, neuronal cells and ovarian cells were all successfully grown on PSi.[148-152] Furthermore, Sun and co-workers reported PSi can even support and promote primary osteoblast growth, protein-matrix synthesis and mineralization for bone tissue-engineering.[153] There are studies showing the inplantation of PSi discs into live animals for tissue engineering. [154-157]
Rosengren *et al.* have studied the *in vivo* tissue compatibility of implanted mesoporous silicon discs in rat abdominal walls. The study showed PSi elicited a certain degree of foreign body reaction consisting of an inner monocytes/macrophages rich zone, but can be used to construct a neural sieve electrode.[156] Johansson *et al.* have found that porous silicon implanted into nervous tissue of rat acted positively as an electrode material for nerve repair without any overt signs of abnormal tissue reaction or toxicity.[157]

PSi has also been shown to degrade completely over time in biological systems, which has opened a route towards implantable devices based on this material.[158] The degradation product is non-toxic orthosilicic acid, the major form of silicon in human body for normal bone and connective tissue homeostasis that is readily excreted *via* the kidneys.[159, 160] The dissolution of PSi can be described as a simplified

two-step process:

$Si(s) + 2H_2O(l) \rightarrow SiO_2(s) + 2H_2(g)$

$SiO_2(s) + 2H_2O(l) \rightarrow Si(OH)_4(l)$

The degradability of PSi has led to the feasibility of *in vivo* applications, for which PSi particles are in favoured. The cytotoxicity of PSi particles on the human colon carcinoma (Caco-2) cells was influenced by surface chemistry and particle size. At particle sizes > 25 μm, the non-toxic threshold concentration for carbonized PSi particles was < 2 mg/mL, and for oxidized particles was < 4 mg/mL.[161] Salonen *et al.* have studied the effects of hydrocarbonized PSi particles on Caco-2 and RAW 264.7 murine macrophage cells in terms of toxicity, oxidative stress and inflammatory response.[162] The particles of the size 142 nm were found to have strong cell membrane interaction, induce less cellular damage than other particle sizes and maintain high levels of cellular ATP production (i.e. cells are metabolically active.) The interaction of PSi particles (nominal diameter of 600 and 1000 nm) with human umbilical vein endothelial cells (HUVECs) and murine J774A.1 macrophages *in vitro* was reported recently. No effect on viability of endothelial cells was recorded for over three days and the level of pro-inflammatory cytokines released from particles-treated macrophages was comparable with that of untreated cells.[133] Similar results were obtained from PSi particles of two different sizes (1.6 and 3.2 μm in diameter) by which endothelial cell morphology, viability and mitotic potential were unaffected and no release of pro-inflammatory cytokines IL-6 and IL-8 in THP1 human macrophages was induced.[163-165]

Further, *in vivo* animal tests were performed on particles to show no damage to healthy cells and tissues. PSi microparticles at the size of 1.6 μm with different chemistry such as oxidized and 3-aminopropyltriethoxysilane modified surfaces were intravenously administered into mice to evaluate the safety of use *in vivo*. These particles did not change the plasma level of renal and hepatic biomarkers, nor lead to infiltration of leukocytes into the liver, spleen, kidney, lung, brain, heart and thyroid.[166] Luminescent PSi particles of the size 126 nm were intravenously injected into mouse to test biodegradability and biocompatibility. The injected luminescent particles accumulated mainly in the liver and spleen and were cleared from the body in 4 weeks due to the degradation into silicic acid followed by excretion. Moreover, no significant toxicity was observed in kidney, liver and spleen tissues 1 day and 4 weeks after particles injection.[167] A compelling example of the suitability of PSi particles for *in vivo* study was illustrated by Cheng and co-workers.[168] When injecting unmodified, oxidized or hydrosilylated PSi particles (10 – 30 μm) into rabbit eyes, no toxicity was observed during a period of more than four months and the particles eventually degraded completely. Low *et al.* also implanted nano-size silanized PSi into rat eyes and found it able to support cell attachment and expansion.[99]

The biodistribution of PSi particles is particularly interesting for *in vivo* sensing applications and drug delivery. Biodistribution study of the particles with the size of 142 nm in rats indicated rapid removal of particles from the circulation after intravenous administration, no absorption through the gastrointestinal tract and particle excretion in fecal pellets after oral administration and that particles resided in the injection site for up to 4 h after subcutaneous administration.[162] Sarparanta *et al.* have examined the distribution of PSi particles at the size range of 1 to 10 μm in rat gastrointestinal (GI) tract after the oral administration. At the two-hour time point, most of particles resided in the stomach. At the four-hour time point, the particles migrated to the ileum. The low accumulation of the radiolabelled particles in bones showed the high stability of these particles in GI tract.[169] Under the intravenous administration, particles were accumulated mostly in the liver and spleen of rats and eventually excreted *via* the kidneys.[170] Decuzzi and co-workers have further investigated the size and shape effects in the biodistribution of intravascularly injected PSi particles in mice.[171] For spherical particles, it has been found that at the size of 0.7 and 1 μm particles provided more uniform tissue distribution than those with sizes at 2.5 and 3 μm. For non-spherical particles, discoidal particles were observed to largely accumulate in most of the organs, except liver, where quasi-hemispherical and cylindrical particles were more easily internalized. In the accumulated sites, the discoidal particles were found to associate mainly with macrophages. Compared with spherical particles, those non-spherical particles were shown to interact more frequently with the vessel walls and thus exhibited significant particle accumulation.[133]

6.2 Drug delivery

Due to the biocompatibility as well as high surface area, tunable pore size and convenient chemical modification on the surface to increase the solubility of poorly soluble payloads, the major application of PSi particles have been in delivery of therapeutic agents, such as drugs and peptides, as carriers.[172-179] We will briefly survey a few of these studies to demonstrate the scope of using PSi particles *in vivo*.

The association of PSi particles as drug carriers with various types of cells *in vitro* were investigated massively. Vascular endothelial cells were capable of rapidly internalizing both positively and negatively charged PSi particles.[163, 164] Following internalization, particles were located in endosome where cellular proliferation, apoptosis, cell cycle and cytokine production were unaltered.[180] Thermally oxidized PSi particles, interacting with Caco-2 epithelial cells and RAW 264.7 macrophages, showed no significant effect on cellular viability. The degradation profile of these particles illustrated that more than 80% of particles were dissolved in biologically relevant media at 6 days.[181] Thermally hydrocarbonized PSi microparticles coated with hydrophobin protein were able to improve their hydrophilicity and further the biocompatibility in drug delivery applications, as cell viability assessment of these particles showed that protein promoted cell viability on

human gastric adenocarcinoma (AGS) cells, Caco-2 cells and human colon adenocarcinoma (HT-29) cells.[182, 183] The particles were also found to be non-cytotoxic and mucoadhesive in human gastric adenocarcinoma (AGS) cells.[184] The same type of thermally carbonized PSi particles loaded with antibiotic ethionamide caused drastic decrease in the toxicity of the drug to cells, as the toxic concentration threshold for ethionamide was lifted from 0.10 mM or 0.25 mM to 0.9 mM for RAW264.7 and Caco-2 cells.[185]

In vivo studies of drug delivery *via* PSi particles were investigated. Tanaka *et al.* provided a multistage delivery system based on PSi particles to transport small interfering RNA (siRNA) for cancer treatment *in vivo*.[186] PSi microparticles as stage 1 vector loaded with nanoliposomes and siRNA were injected into mice bearing ovarian tumors. The results evidenced an effective therapeutic effect of the multistage siRNA delivery in two mouse models of human ovarian cancer, but no observable concurrent toxicity, no significant level of inflammatory cytokines and no tissue injury in the kidney, liver and spleen of mice were observed. Kilpeläinen *et al.* demonstrated the sustained delivery of peptides Melanotan II and ghrelin antagonist to rats and mice *via* thermally hydrocarbonized nanoPSi microparticles.[187, 188] It was reported that released peptides remained pharmacologically active and the PSi microparticles did not increase plasma cytokine concentration acutely, suggesting a safe material for effective drug delivery.[187] Some of the most advanced clinical studies have been performed by pSiMedica, inc. (now pSivida), using PSi as a brachytherapy device for liver cancer treatment on a first-in-man study.[189] The PSi particles with a proven anticancer therapeutic, radioactive isotope 32-phosphorus were implanted locally into patients' livers and patients were monitored for up to 24 weeks. The result showed no clinically significant adverse events and no trends in serum biochemistry or hematology data with PSi implantation, and suggested the ability of PSi to perform *in vivo* drug delivery with no harm to the human body.

6.3 PSi photonic microparticles

A classic way of synthesizing PSi particles is fracture of freestanding PSi film to small particles (so-called "smart dust") *via* ultrasonication [190] or by ball milling[191]. These smart dusts particles are random in size typically ranging from a few micrometers to a few nanometers but generally display the same optical properties as the freestanding film. Link and Sailor have reported bifunctional PSi photonic crystal particles by sonicating the PSi films with both hydrophobic and hydrophilic characters. These particles are able to self-assemble and self-organize themselves, which can be monitored by the optical shifts in the reflectivity spectra.[192] The shattered PSi particles, maintaining the same self-reporting optical properties as PSi films, are also compatible with surface modifications. It was demonstrated that particles can be covalently modified with antibodies such that they can specifically bind to biomolecules, opening a way towards cell-based sensing (Figure 13).[12] PSi particles can also be functionalized with biotin and then bind to avidin-modified PSi Bragg mirror, forming self-assembled optical resonant microcavities.[46]

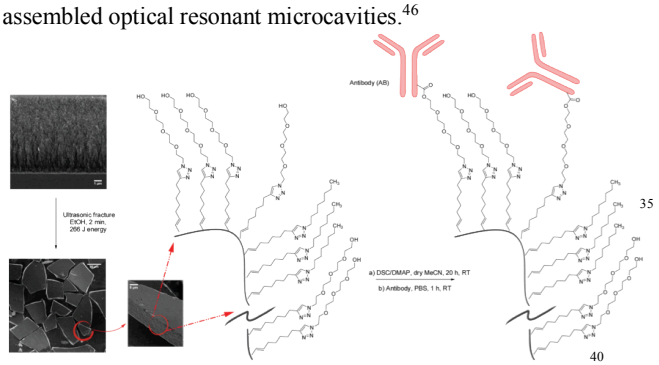

Figure 13 The fabrication of PSi particles *via* ultrasonication of freestanding PSi film and the surface functionalisation approach for immobilisation of antibodies on the exterior surfaces of PSi particles. Briefly, the distal alcohol moieties on the tetra(ethylene glycol) modified surfaces were converted to succinimide esters using DSC (*N,N'*-disuccinimidyl carbonate) linker, which then allowed covalent coupling of amine groups from lysine residues of antibodies.[12](Reproduced from Ref. 12 with permission from The Royal Society of Chemistry).

"Smart dust" has been used in sensing applications from the very beginning of their development. Sailor and co-workers utilized the particles with a sharp maximum in the reflectivity spectra for detection of volatile organic compounds by measuring the optical shifts.[193, 194] PSi photonic crystal particles with encoded optical features in the reflectivity spectrum have been applied in biological screening test. Particles modified with rat albumin or with bovine serum albumin could be differentiated from each other *via* fluorescence and reflectivity spectral change, caused by interaction with primary rabbit anti-rat-albumin antibody followed by FITC- (fluorescein isothiocyanate) conjugated goat anti-rabbit immunoglobulin-G.[195] Recent work in drug delivery has demonstrated that the optical and spectral changes in PSi particles can monitor particle degradation and drug release in real time *in vitro*.[196] As drugs are released from the pores of PSi particles, causing the refractive index change, blue shifts in spectra or colour change in particles can be observed. In the same manner, these photonic crystal particles are able to detect cellular secretion and changes in cellular circumstance by optical shifts.

However, particles prepared *via* ultrasonication or ball milling share the disadvantage that the shape and size of particles cannot be well controlled. As the uniformity and reproducibility of particles' geometry are important for *in vivo* sensing applications, monodisperse PSi

particles with tunable pore morphology are desired.

6.4 From microfabrication to PSi particles

Microfabrication of PSi leads to the synthesis of freestanding PSi photonic crystal particles with uniform shape and size. Li and co-workers have fabricated PSi particles with unique optical features by soft lithography with poly-dimethylsiloxane (PDMS) stamps and a polymer "ink".[197] The generated particles consist of a pristine PSi moiety capable of optical sensing and a polymer infused moiety as a mechanical scaffold and an internal reference point/ an optical barcode in sensing process. Yet no sensing application of these polymer-contained PSi particles has been reported. Meade and Sailor have reported a method to microfabricate PSi particles by patterning electrochemically prepared PSi film, removing redundant PSi with reactive ion etch and then lifting particles off the substrate *via* electropolishing.[134] The resulting particles with disc shapes and uniform sizes containing "spectral barcodes" (i.e. exhibiting several peaks in the reflectivity spectrum) are of interest for sensing applications, as it was demonstrated that such encoded structure could be used as vapour sensors and self-reporting materials.[198] A sensing example of the spectrally encoded particles was demonstrated on multiplexed DNA detection.[124] Si encoded particles were oxidized, modified with a silane linker and conjugated to various oligonucleotide probes. When DNA binding assays were performed on the particles, changing the optical properties, the reflectivity spectra of the particles can be decoded to obtain the multiple DNA information.

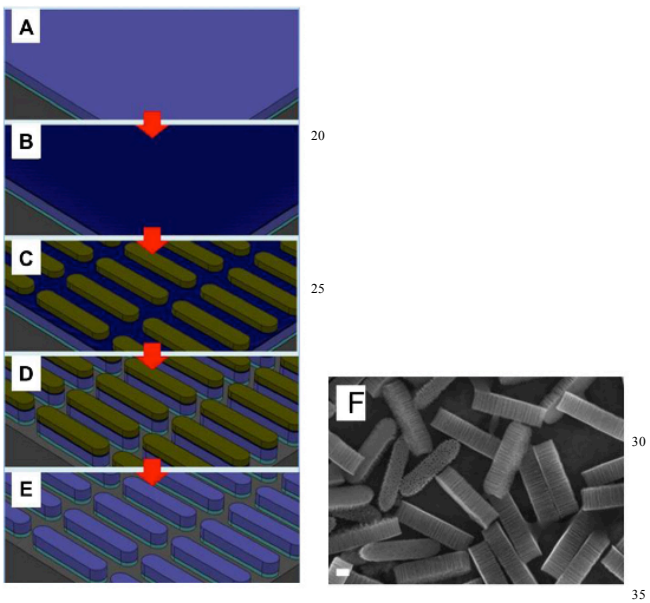

Figure 14 The fabrication process of rod-like mesoporous silicon particles *via* standard photolithography: A) PSi (light blue) film with a high porosity release layer (cyan) at the bottom of the structure. B) Capping of the film with a low temperature oxide layer (dark blue). C) Photolithographic patterning of the particle array with a custom-designed mask. D) Reactive ion etching to remove undesired part of PSi. E) Stripping of the photoresist and oxide layer to yield arrays of rod-like particles. F) Scanning electronic microscope (SEM) image of PSi rods after release from the substrate by sonication. Scale bar = 200 nm. (Reproduced with permission from Ref. 202. Copyright (2012) Elsevier).

More complicated shapes than disks of PSi particles were demonstrated by Ferrari and co-workers.[199] Bowl-shaped PSi particles with particle and pore size precisely tailored by electrochemical etch process were fabricated *via* standard photolithography.[108] A silicon nitride layer followed by a layer of photoresist was first deposited on silicon wafer. By means of contact photolithography and several dry or wet etching, the pattern was formed on nitride layer with trenches in silicon substrate. Electrochemical etch was then performed to produce bowl-like PSi particles. These bowl-shaped particles have been largely applied to the multi-stage drug delivery system,[200] which will be discussed in the following section. Recently, a different strategy of microfabricating uniform PSi particles by patterning on PSi film instead of silicon substrate was reported.[201, 202] In the process, the particle porosity and pore size were controlled by electrochemical etching, while particle dimension was independently defined by photolithography. Therefore, discoidal and rod-like mesoporous silicon particles can be easily fabricated (Figure 14).[202] Comparison was also made among different shapes of particles in the adhesion ability in flow chamber system. The results showed that disc-like particles adhered longer than the other two, and were expected to be more effective in targeting in microvascular environment for drug delivery purpose. Though this fabrication technique provides fine-tailored monodisperse particles in size, shape, porosity, pore size and morphology, a disadvantage of these particles is that they often do not have the featured optical properties to be applied in sensing applications or controlled drug delivery. Thus other nanoparticles were engineered into the PSi particles, producing a hybrid system for various purposes.

6.5 Hybrid particles

Beside the unique optical properties, PSi particles can be engineered with other metal nanoparticles inside the pores, to allow two or more properties combined in a single particle for future applications.

A typical type of hybrid PSi particles was fabricated by infusing superparamagnetic nanoparticles of Fe_3O_4 into the hydrophilic layer of amphiphilic PSi photonic crystal film and conducting sonication.[203] The resulting particles can be used to manipulate and monitor small volumes of liquids such as enzymatic payload and oligonucleotides as in a microfluidic system, for the orientation of particles can be controlled by magnetic field to achieve the loading and delivery of liquid and the whole process can be monitored by the reflectivity spectrum.[204, 205] Similarly, metal nanoparticles were also incorporated into PSi particles with photoluminescence. Gu *et al.* demonstrated "smart" PSi particles engineered with both fluorescent and magnetic functions to achieve fluorescent tracking and localized delivery of a drug under the guidance of a magnetic field to cancer cells *in vitro*.[206] Munoz-Noval *et al.* reported a method to infiltrate Co and Fe nanoparticles into luminescent PSi particles, which can be internalized into human mesenchymal stem cells with no apoptosis induction.[207,208] Thus cellular tracking or sensing through fluorescence of particles might be achieved.

Ferrari and co-workers conducted a series of studies on PSi particles loaded with different types of nanoparticles in the application of drug delivery, so called multi-stage drug delivery stystem.[200] PSi particles play the roles of nanocarriers taken up by cells of different tissues, protecting active agents (i.e. various types of nanoparticles) inside the pores from exposure to the unstable factors, such as degradation of enzyme. The nanoparticles loaded within PSi then act as imaging, therapeutic agents or higher order carriers. For example, quantum dots (Q-dots) and fluophor-labelled single-wall carbon nanotubes (SWNTs) were engineered into the pores of PSi particles for delivery to human vascular cells *in vitro*. Fluorescence imaging confirmed the internalization and accumulation of Q-dots and SWNTs in cells under the protection of PSi particles.[209] Superparamagnetic iron oxide nanoparticles were also demonstrated to present inside the PSi particles for partitioning particles into unique cellular locations by different functional groups on the nanoparticles.[210] It is credible that by integrating optical reflectance of PSi and other properties from nanoparticles, the hybrid PSi particles might represent powerful sensing tools towards *in vivo* cellular applications.

7. Summary and prospects

The development of PSi photonic crystals for biosensing applications has progressed enormously since the seminal paper by Lin *et al.* just 15 years ago. After some initial promise PSi as a biosensing material seemed to progress slowly until some major developments in surface chemistry gave researchers an ability to stabilise the material in aqueous media as well as provide antifouling capabilities and attach specific recognition molecules. Other important advances were developments in fabricating more sophisticated optical structures, the microfabrication of PSi into well-defined sensing domains or even microparticles and the demonstration that PSi microparticles could be used *in vivo* with minimal impact on the host organism. These advances have seen PSi begin to emerge as a powerful tool for fabricating protein and cell arrays and for applications as *in vivo* sensors. We certainly feel the demonstrated ability to configure PSi photonic crystals to detect protease activity in cell culture and from captured cells gives PSi enormous potential for *in vivo* monitoring of infection and macrophage cell activity as well as for making cell chips. With the application of PSi as a drug delivery agent as well there also exists the exciting potential of using PSi as a self-reporting drug delivery vehicle that could provide the user an indication of when drugs are being released. Accompanied with the advanced in fabrication and modification of PSi are advances in microfluidics where PSi could be used as a detector in an integrated microfluidic analytical system for monitoring cellular behaviour. We expect some very exciting developments in the application of PSi in biosensors, especially live cell biosensing, within the next few years.

References

1. L. T. Canham, *Applied Physics Letters*, 1990, **57**, 1046.
2. G. Vincent, *Applied Physics Letters*, 1994, **64**, 2367-2369.
3. L. T. Canham, *Adv. Mater.*, 1995, **7**, 1033-1037.
4. V. S. Y. Lin, K. Motesharei, K.-P. S. Dancil, M. J. Sailor and M. R. Ghadiri, *Science*, 1997, **278**, 840-843.
5. S. Ilyas, T. Böcking, K. Kilian, P. J. Reece, J. Gooding, K. Gaus and M. Gal, *Optical Materials*, 2007, **29**, 619-622.
6. K. A. Kilian, T. Boecking and J. J. Gooding, *Chemical Communications*, 2009, 630-640.
7. J. M. Buriak, *Chemical Reviews*, 2002, **102**, 1271-1308.
8. S. Ciampi, J. B. Harper and J. J. Gooding, *Chem. Soc. Rev.*, 2010, **39**, 2158-2183.
9. M. P. Stewart and J. M. Buriak, *Advanced Materials*, 2000, **12**, 859-869.
10. S. D'Auria, M. de Champdore, V. Aurilia, A. Parracino, M. Staiano, A. Vitale, M. Rossi, I. Rea, L. Rotiroti, A. M. Rossi, S. Borini, I. Rendina and L. De Stefano, *Journal of Physics: Condensed Matter*, 2006, **18**, S2019-S2028.
11. A. Jane, R. Dronov, A. Hodges and N. H. Voelcker, *Trends Biotechnol.*, 2009, **27**, 230-239.
12. B. Guan, A. Magenau, K. A. Kilian, S. Ciampi, K. Gaus, P. J. Reece and J. J. Gooding, *Faraday Discussions*, 2011, **149**, 301-317.
13. K. A. Kilian, L. M. H. Lai, A. Magenau, S. Cartland, T. Bocking, G. N. Di, M. Gal, K. Gaus and J. J. Gooding, *Nano Lett.*, 2009, **9**, 2021-2025.

14. L. Canham, in *Properties of Porous Silicon*, Institution of Engineering and Technology, London, 1997, pp. 1-29.
15. R. L. Smith and S. D. Collins, *Journal of Applied Physics*, 1992, **71**, R1-R22.
16. É. Vázsonyi, E. Szilágyi, P. Petrik, Z. E. Horváth, T. Lohner, M. Fried and G. Jalsovszky, *Thin Solid Films*, 2001, **388**, 295-302.
17. A. G. Cullis, L. T. Canham and P. D. J. Calcott, *Applied Physics Reviews*, 1997, **82**, 909-956.
18. W. Theiß, *Surface Science Reports*, 1997, **29**, 91-192.
19. N. Kunzner, D. Kovalev, J. Diener, E. Gross, V. Y. Timoshenko, G. Polisski, F. Koch and M. Fujii, *Opt. Lett.*, 2001, **26**, 1265-1267.
20. M. G. Berger, C. Dieker, M. Thonissen, L. Vescan, H. Luth, H. Munder, W. Theiss, M. Wernke and P. Grosse, *Journal of Physics D: Applied Physics*, 1994, **27**, 1333.
21. W. H. Zheng, P. Reece, B. Q. Sun and M. Gal, *Applied Physics Letters*, 2004, **84**, 3519-3521.
22. A. Bruyant, G. Lérondel, P. J. Reece and M. Gal, *Applied Physics Letters*, 2003, **82**, 3227-3229.
23. P. J. Reece, G. Lerondel, W. H. Zheng and M. Gal, *Applied Physics Letters*, 2002, **81**, 4895-4897.
24. J. Rouquerol, D. Avnir, C. W. Fairbridge, D. H. Everett, J. H. Haynes, N. Pernicone, J. D. F. Ramsay, K. S. W. Sing and K. K. Unger, *Pure and Applied Chemistry*, 1994, **66**, 1739-1758.
25. M. M. Orosco, C. Pacholski, G. M. Miskelly and M. J. Sailor, *Adv. Mater. (Weinheim, Ger.)*, 2006, **18**, 1393-1396.
26. L. De Stefano, I. Rendina, L. Moretti, S. Tundo and A. M. Rossi, *Applied Optics*, 2004, **43**, 167-172.
27. S. Chan, P. M. Fauchet, Y. Li, L. J. Rothberg and B. L. Miller, *Physica Status Solidi A: Applied Research*, 2000, **182**, 541-546.
28. C. Pacholski, M. Sartor, M. J. Sailor, F. Cunin and G. M. Miskelly, *Journal of the American Chemical Society*, 2005, **127**, 11636-11645.
29. L. A. DeLouise and B. L. Miller, *SPIE Proceedings*, 2004, **5357**, 111-125.
30. H. Ouyang, M. Christophersen, R. Viard, B. L. Miller and P. M. Fauchet, *Advanced Functional Materials*, 2005, **15**, 1851-1859.
31. X. Wei, C. Kang, M. Liscidini, G. Rong, S. T. Retterer, M. Patrini, J. E. Sipe and S. M. Weiss, *Journal of Applied Physics*, 2008, **104**.
32. X. Wei and S. M. Weiss, *Optics express*, 2011, **19**, 11330-11339.
33. A. M. Rossi, S. Borini, L. Boarino and G. Amato, *physica status solidi (a)*, 2003, **197**, 284-287.
34. G. Lérondel and R. Romestain, *Thin Solid Films*, 1997, **297**, 114-117.
35. A. Loni, L. T. Canham, M. G. Berger, R. Arens-Fischer, H. Munder, H. Luth, H. F. Arrand and T. M. Benson, *Thin Solid Films*, 1996, **276**, 143-146.
36. H. F. Arrand, T. M. Benson, A. Loni, R. Arens-Fischer, M. G. Krueger, M. Thoenissen, H. Lueth, S. Kershaw and N. N. Vorozov, *Journal of Luminescence*, 1998, **80**, 119-123.
37. J. D. Ryckman, M. Liscidini, J. E. Sipe and S. M. Weiss, *Applied Physics Letters*, 2010, **96**.
38. G. Rong, J. D. Ryckman, R. L. Mernaugh and S. M. Weiss, *Applied Physics Letters*, 2008, **93**.
39. G. Lerondel, R. Romestain, J. C. Vial and M. Thonissen, *Applied Physics Letters*, 1997, **71**, 196-198.
40. E. Guillermain, V. Lysenko, R. Orobtchouk, T. Benyattou, S. Roux, A. Pillonnet and P. Perriat, *Applied Physics Letters*, 2007, **90**.
41. C. Jamois, C. Li, R. Orobtchouk and T. Benyattou, *Photonics and Nanostructures - Fundamentals and Applications*, 2010, **8**, 72-77.
42. H. Qiao, B. Guan, J. J. Gooding and P. J. Reece, *Optics express*, 2010, **18**, 15174-15182.
43. F. Michelotti, B. Sciacca, L. Dominici, M. Quaglio, E. Descrovi, F. Giorgis and F. Geobaldo, *Physical Chemistry Chemical Physics*, 2010, **12**, 502-506.
44. H. Qiao, B. Guan, T. B√∂cking, M. Gal, J. J. Gooding and P. J. Reece, *Applied Physics Letters*, 2010, **96**.
45. T. B√∂cking, K. A. Kilian, P. J. Reece, K. Gaus, M. Gal and J. J. Gooding, *ACS Applied Materials and Interfaces*, 2010, **2**, 3270-3275.
46. T. Bocking, K. A. Kilian, P. J. Reece, K. Gaus, M. Gal and J. J. Gooding, *Soft Matter*, 2011.
47. K. A. Kilian, T. Böcking, K. Gaus, M. Gal and J. J. Gooding, *Biomaterials*, 2007, **28**, 3055-3062.
48. K. A. Kilian, T. Böcking, S. Ilyas, K. Gaus, M. Gal and J. J. Gooding, *Advanced Functional Materials*, 2007, **17**, 2884-2890.
49. S. Chan, S. R. Horner, P. M. Fauchet and B. L. Miller, *Journal of the American Chemical Society*, 2001, **123**, 11797-11798.
50. M. Archer, M. Christophersen and P. M. Fauchet, *Biomedical Microdevices*, 2004, **6**, 203-211.
51. C. Steinem, A. Janshoff, V. S. Y. Lin, N. H. Voelcker and G. M. Reza, *Tetrahedron*, 2004, **60**, 11259-11267.
52. K.-P. S. Dancil, D. P. Greiner and M. J. Sailor, *Journal of the American Chemical Society*, 1999, **121**, 7925-7930.
53. L. M. Bonanno and L. A. DeLouise, *Langmuir*, 2007, **23**, 5817-5823.
54. M. P. Schwartz, S. D. Alvarez and M. J. Sailor, *Analytical Chemistry*, 2007, **79**, 327-334.
55. L. A. DeLouise, P. M. Kou and B. L. Miller, *Analytical Chemistry*, 2005, **77**, 3222-3230.
56. R. R. K. Reddy, A. Chadha and E. Bhattacharya, *Biosensors & Bioelectronics*, 2001, **16**, 313-317.
57. S. E. Letant, B. R. Hart, S. R. Kane, M. Z. Hadi, S. J. Shields and J. G. Reynolds, *Adv. Mater.*, 2004, **16**, 689-693.
58. S. E. Letant, S. R. Kane, B. R. Hart, M. Z. Hadi, T.-C. Cheng, V. K. Rastogi and J. G. Reynolds, *Chemical Communications (Cambridge, United Kingdom)*, 2005, 851-853.
59. P. S. Chaudhari, A. Gokarna, M. Kulkarni, M. S. Karve and S. V. Bhoraskar, *Sensors and Actuators, B: Chemical*, 2005, **B107**, 258-263.
60. M. R. Linford and C. E. D. Chidsey, *J. Am. Chem. Soc.*, 1993, **115**, 12631-12632.
61. M. R. Linford, P. Fenter, P. M. Eisenberger and C. E. D. Chidsey, *J. Am. Chem. Soc.*, 1995, **117**, 3145-3155.
62. L. H. Lie, S. N. Patole, A. R. Pike, L. C. Ryder, B. A. Connolly, A. D. Ward, E. M. Tuite, A. Houlton and B. R. Horrocks, *Faraday Discuss FIELD Full Journal Title:Faraday discussions*, 2004, **125**, 235-249; discussion 293-309.
63. B. R. Hart, S. E. Letant, S. R. Kane, M. Z. Hadi, S. J. Shields and J. G. Reynolds, *Chem. Commun.*, 2003, **3**, 322-323.

64. K. A. Kilian, T. Böcking, K. Gaus, M. Gal and J. J. Gooding, *ACS Nano*, 2007, submitted.
65. S. Ciampi, T. Böcking, K. A. Kilian, J. B. Harper and J. J. Gooding, *Langmuir*, 2008, **24**, 5888-5892.
66. K. A. Kilian, T. Böcking, K. Gaus, J. King-lacroix, M. Gal and J. J. Gooding, *Chemical Communications*, 2007, 1936-1938.
67. K. A. Kilian, T. Böcking, K. Gaus and J. J. Gooding, *Angewandte Chemie International Edition*, 2008, **47**, 2697-2699.
68. T. Böcking, K. A. Kilian, K. Gaus and J. J. Gooding, *Langmuir*, 2006.
69. T. Böcking, M. Gal, K. Gaus and J. J. Gooding, *Australian Journal of Chemistry*, 2005, **58**, 660-663.
70. T. Böcking, K. A. Kilian, J. J. Gooding and M. Gal, *Nature Photonics*, 2008, **Submitted**.
71. S. Ciampi, T. Böcking, K. A. Kilian, M. James, J. B. Harper and J. J. Gooding, *Langmuir*, 2007, **23**, 9320-9329.
72. S. Chan, S. R. Horner, P. M. Fauchet and B. L. Miller, *J. Am. Chem. Soc.*, 2001, **123**, 11797-11798.
73. V. M. Starodub, L. L. Fedorenko, A. P. Sisetskiy and N. F. Starodub, *Sens. Actuators, B*, 1999, **B58**, 409-414.
74. L. M. a. D. Bonanno, L.A. , *Biosens. Bioelectron.*, 2007, **23**, 444.
75. L. M. Bonanno, T. C. Kwong and L. A. DeLouise, *Analytical Chemistry*, 2010, **82**, 9711-9718.
76. L. M. D. Bonanno, L. A. , *Anal. Chem.* , 2010, **82**, 714-722.
77. L. A. DeLouise and B. L. Miller, *Analytical Chemistry*, 2004, **76**, 6915-6920.
78. L. A. DeLouise and B. L. Miller, *Analytical Chemistry*, 2005, **77**, 1950-1956.
79. T. B. c. Kristopher A. Kilian, Katharina Gaus, Michael Gal, and J. Justin Gooding, *ACS Nano*, 2007, **1**, 355-361.
80. M. e. a. Orosco, *Adv. Mater. (Weinheim, Ger.)*, 2006, **18**, 1393.
81. M. M. Orosco, C. Pacholski and M. J. Sailor, *Nat. Nanotechnol.*, 2009, **4**, 255-258.
82. K. A. Kilian, T. Böcking, K. Gaus and J. J. Gooding, *ACS Nano*, 2007, **1**, 355-361.
83. R. H. U. L. J. Jones, R. P. Haugland, N. Panchuk-Voloshina, M. Zhou, R. P. Haugland, *Anal. Biochem.* , 1997, **251**, 144.
84. W. T. R. Wiesner, *Anal. Biochem.* , **121**, 290.
85. J. M. L. Anson, *Gen. Physiol.*, 1938, **22**, 79.
86. V. C. O. Folin, *J. Biol. Chem.*, **73**, 627.
87. M. S. W. W. P. Esler, *Science*, 2001, **293**, 1449.
88. L. J. S. C. A. Hart, S. Bagley, A. A. G. Bryden, N. W. Clarke, S. H. Lang *Br. J. Cancer* 2002, **86**, 1136.
89. B. D. B. R. Vassar, S. Babu-Khan, S. Kahn, E. A. Mendiaz, and D. B. T. P. Denis, S. Ross, P. Amarante, R. Loeloff, Y. Luo, S. Fisher, J. Fuller, S. Edenson, J. Lile, M. A. Jarosinski, A. L. Biere, E. Curran, T. Burgess, J. C. Louis, F. Collins, J. Treanor, G. Rogers, M. Citron, *Science*, 1999, **286**, 735.
90. F. A. K. D. Bidle, *Nature*, 1999, **397**, 508.
91. S. S. M. K. R. Klimpel, G. Thomas, S. H. Leppla, , *Proc. Natl. Acad. Sci. USA* 1992, **89**, 10277.
92. B. J. Stewart MP, *Advanced Materials*, 2000, **12**, 859-869.
93. S. M. Le´tant S, *Advanced Materials* 2000, **12**, 355-359.
94. F. P. Chan S, Li Y, Rothberg LJ, Miller BL. , *Physica Status Solidi (A)*, 2000, **182**, 541-546.
95. D. K. Janshoff A, Steinem C, Greiner DP, Lin VSY, Gurtner C, et al. , *Journal of American Chemical Society*, 1998, **120**, 12108-12116.
96. H. B. Le´tant SE, Kane SR, Hadi MZ, Shields SJ, Reynolds JG. , *Advanced Materials*, 2004, **16**, 689-693.
97. C. B. Chin V, Sailor MJ, Bhatia SN. , *Adv. Mater. (Weinheim, Ger.)*, 2001, **13**, 1877-1880.
98. S. P. Low, K. A. Williams, L. T. Canham and N. H. Voelcker, *Biomaterials*, 2006, **27**, 4538-4546.
99. S. P. Low, N. H. Voelcker, L. T. Canham and K. A. Williams, *Biomaterials*, 2009, **30**, 2873-2880.
100. S. D. Alvarez, M. P. Schwartz, B. Migliori, C. U. Rang, L. Chao and M. J. Sailor, *Phys. Status Solidi A*, 2007, **204**, 1439-1443.
101. M. P. e. a. Schwartz, *Langmuir*, 2006, **22**, 7084-7090.
102. K. A. Kilian, T. Böcking, L. M. H. Lai, S. Ilyas, K. Gaus, M. Gal and J. J. Gooding, *International Journal of Nanotechnology*, 2007, **5**, 170-178.
103. A. Jane, R. Dronov, A. Hodges and N. H. Voelcker, *Trends Biotechnol*, 2009, **27**, 230-239.
104. J. R. Dorvee, M. J. Sailor and G. M. Miskelly, *Dalton Transactions*, 2008, 721-730.
105. L. Chen, Z.-T. Chen, J. Wang, S.-J. Xiao, Z.-H. Lu, Z.-Z. Gu, L. Kang, J. Chen, P.-H. Wu, Y.-C. Tang and J.-N. Liu, *Lab on a Chip*, 2009, **9**, 756-760.
106. B. S. Flavel, M. J. Sweetman, C. J. Shearer, J. G. Shapter and N. H. Voelcker, *Acs Applied Materials & Interfaces*, 2011, **3**, 2463-2471.
107. F. Cunin, T. A. Schmedake, J. R. Link, Y. Y. Li, J. Koh, S. N. Bhatia and M. J. Sailor, *Nature Materials*, 2002, **1**, 39-41.
108. C. Chiappini, E. Tasciotti, J. R. Fakhoury, D. Fine, L. Pullan, Y.-C. Wang, L. Fu, X. Liu and M. Ferrari, *ChemPhysChem*, 2010, **11**, 1029-1035.
109. S. Borini, *Journal of The Electrochemical Society*, 2005, **152**, G482-G486.
110. H.-F. Li, H.-M. Han, Y.-G. Wu and S.-J. Xiao, *Applied Surface Science*, 2010, **256**, 4048-4051.
111. M. Krüger, R. Arens-Fischer, M. Thönissen, H. Münder, M. G. Berger, H. Lüth, S. Hilbrich and W. Theiss, *Thin Solid Films*, 1996, **276**, 257-260.
112. H. Kim, K. Chong and Y. Xie, *Applied Physics Letters*, 2003, **83**, 28710.
113. R.-t. Yamaguchi, K.-i. Miyamoto, K.-i. Ishibashi, A. Hirano, S. M. Said, Y. Kimura and M. Niwano, *Journal of Applied Physics*, 2007, **102**, 014303-014307.
114. N. Tokranova, D. Song, A. Gracias and J. Castracane, San Jose, CA, USA, 2007.
115. I. Rea, A. Lamberti, I. Rendina, G. Coppola, M. Gioffre, M. Iodice, M. Casalino, E. De Tommasi and L. De Stefano, *Journal of Applied Physics*, 2010, **107**, 014513-014514.

116.Y. Harada, X. Li, P. W. Bohn and R. G. Nuzzo, *Journal of the American Chemical Society*, 2001, **123**, 8709-8717.
117.Z. Mohammad, K. Mahdi, E. Alireza and R. Farshid, *Journal of Micromechanics and Microengineering*, 2011, **21**, 065006.
118.I. S. Chun, E. K. Chow and X. Li, *Applied Physics Letters*, 2008, **92**, 191113-191113.
119.J. Ji, X. Li, L. T. Canham and J. L. Coffer, *Advanced Materials*, 2002, **14**, 41-43.
120.V. V. Doan and M. J. Sailor, *Applied Physics Letters*, 1992, **60**, 619-620.
121.M. J. Sweetman, M. Ronci, S. R. Ghaemi, J. E. Craig and N. H. Voelcker, *Advanced Functional Materials*, 2012, **22**, 1158-1166.
122.M. J. Sweetman, C. J. Shearer, J. G. Shapter and N. H. Voelcker, *Langmuir*, 2011, 9497-9503.
123.S. O. Meade and M. J. Sailor, *Phys Status Solidi-R*, 2007, **1**, R71-R73.
124.S. O. Meade, M. Y. Chen, M. J. Sailor and G. M. Miskelly, *Analytical Chemistry*, 2009, **81**, 2618-2625.
125.R. Arens-Fischer, M. Krüger, M. Thönissen, V. Ganse, D. Hunkel, M. Marso and H. Lüth, *Journal of Porous Materials*, 2000, **7**, 223-225.
126.C. Jamois, *New Concepts of Integrated Photonic Biosensors Based on Porous Silicon*
127.L. Meifang, G. Parish, L. Yinong, J. M. Dell and A. J. Keating, *Microelectromechanical Systems, Journal of*, 2011, **20**, 418-423.
128.M. P. Stewart and J. M. Buriak, *Angewandte Chemie International Edition*, 1998, **37**, 3257-3260.
129.Y.-L. Khung, S. D. Graney and N. H. Voelcker, *Biotechnology Progress*, 2006, **22**, 1388-1393.
130.T. H. Park and M. L. Shuler, *Biotechnology Progress*, 2003, **19**, 243-253.
131.J. D. Ryckman, M. Liscidini, J. E. Sipe and S. M. Weiss, *Nano Letters*, 2010, **11**, 1857-1862.
132.J. Henri and et al., *Journal of Micromechanics and Microengineering*, 1996, **6**, 14.
133.B. Godin, C. Chiappini, S. Srinivasan, J. F. Alexander, K. Yokoi, M. Ferrari, P. Decuzzi and X. Liu, *Advanced Functional Materials*, 2012, n/a-n/a.
134.S. O. Meade and M. J. Sailor, *phys. stat. sol. (RRL)*, 2007, **1**, R71-R73.
135.X. Sun and C.-z. Li, in *Smart Biosensor Technology*, CRC Press, 2006, pp. 291-334.
136.C. Jianrong, M. Yuqing, H. Nongyue, W. Xiaohua and L. Sijiao, *Biotechnology Advances*, 2004, **22**, 505-518.
137.J. Lei and H. Ju, *Wiley Interdisciplinary Reviews: Nanomedicine and Nanobiotechnology*, 2010, **2**, 496-509.
138.F. Patolsky, G. Zheng and C. M. Lieber, *Analytical Chemistry*, 2006, **78**, 4260-4269.
139.Y. Li, H. Schluesener and S. Xu, *Gold Bulletin*, 2010, **43**, 29-41.
140.L. T. Canham, *Adv. Mater.*, 1995, **7**, 1033-1037.
141.L. T. Canham, C. L. Reeves, D. O. King, P. J. Branfield, J. G. Crabb and M. C. L. Ward, *Adv. Mater.*, 1996, **8**, 850-852.
142.C. Steinhauer, A. Ressine, G. Marko-Varga, T. Laurell, C. A. K. Borrebaeck and C. Wingren, *Anal. Biochem.*, 2005, **341**, 204-213.
143.S. C. Bayliss, R. Heald, D. I. Fletcher and L. D. Buckberry, *Adv. Mater.*, 1999, **11**, 318-321.
144.A. V. Sapelkin, S. C. Bayliss, B. Unal and A. Charalambou, *Biomaterials*, 2006, **27**, 842-846.
145.K. A. Moxon, S. Hallman, A. Aslani, N. M. Kalkhoran and P. I. Lelkes, *J. Biomater. Sci., Polym. Ed.*, 2007, **18**, 1263-1281.
146.S. Bayliss, P. Harris, L. Buckberry and C. Rousseau, *Journal of Materials Science Letters*, 1997, **16**, 737-740.
147.V. Chin, B. E. Collins, M. J. Sailor and S. N. Bhatia, *Adv. Mater.*, 2001, **13**, 1877-1880.
148.A. Angelescu, I. Kleps, M. Mihaela, M. Simion, T. Neghina, S. Petrescu, N. Moldovan, C. Paduraru and A. Raducanu, *Reviews on Advanced Materials Science*, 2003, **5**, 440-449.
149.S. B.-T. de-Leon, A. Sa'ar, R. Oren, M. E. Spira and S. Yitzchaik, *Appl. phys. lett.*, 2004, **84**, 4361-4363.
150.S. P. Low, K. A. Williams, L. T. Canham and N. H. Voelcker, *Biomaterials*, 2006, **27**, 4538-4546.
151.S. Alvarez, A. Derfus, M. Schwartz, S. Bhatia and M. Sailor, *Biomaterials*, 2009, **30**, 26-34.
152.S. C. Bayliss, L. D. Buckberry, I. Fletcher and M. J. Tobin, *Sensors and Actuators A: Physical*, 1999, **74**, 139-142.
153.W. Sun, J. E. Puzas, T.-J. Sheu, X. Liu and P. M. Fauchet, *Adv. Mater.*, 2007, **19**, 4.
154.A. Bowditch, K. Waters, H. Gale, P. Rice, E. Scott, L. Canham, C. Reeves, A. Loni and T. Cox, 1999.
155.J. Coffer, M. Whitehead, D. Nagesha, P. Mukherjee, G. Akkaraju, M. Totolici, R. Same and L. Canham, *Physica Status Solidi(a)*, 2005, **202**, 1451-1455.
156.A. Rosengren, L. Wallman, M. Bengtsson, T. Laurell, N. Danielsen and L. M. Bjursten, *Phys. Status Solidi (a)*, 2000, **182**, 527-531.
157.F. Johansson, L. Wallman, N. Danielsen, J. Schouenborg and M. Kanje, *Acta Biomaterialia*, 2009, **5**, 2230-2237.
158.A. H. Mayne, S. C. Bayliss, P. Barr, M. Tobin and L. D. Buckberry, *phys. stat. sol. (a)*, 2000, **182**, 505-513.
159.D. M. Reffitt, R. Jugdaohsingh, R. P. H. Thompson and J. J. Powell, *J. Inorg. Biochem.*, 1999, **76**, 141-147.
160.S. H. C. Anderson, H. Elliott, D. J. Wallis, L. T. Canham and J. J. Powell, *physica status solidi (a)*, 2003, **197**, 331-335.
161.H. A. Santos, J. Riikonen, J. Salonen, E. Mäkilä, T. Heikkilä, T. Laaksonen, L. Peltonen, V.-P. Lehto and J. Hirvonen, *Acta Biomaterialia*, 2010, **6**, 2721-2731.
162.L. M. Bimbo, M. Sarparanta, H. l. A. Santos, A. J. Airaksinen, E. Mäkilä, T. Laaksonen, L. Peltonen, V.-P. Lehto, J. Hirvonen and J. Salonen, *ACS Nano*, 2010.
163.R. E. Serda, J. Gu, R. C. Bhavane, X. Liu, C. Chiappini, P. Decuzzi and M. Ferrari, *Biomaterials*, 2009, **30**, 2440-2448.
164.R. E. Serda, J. Gu, J. K. Burks, K. Ferrari, C. Ferrari and M. Ferrari, *Cytometry Part A*, 2009, **75A**, 752-760.
165.B. Godin, J. Gu, R. E. Serda, R. Bhavane, E. Tasciotti, C. Chiappini, X. Liu, T. Tanaka, P. Decuzzi and M. Ferrari, *Journal of Biomedical Materials Research Part A*, 2010, **94A**, 1236-1243.

166.T. Tanaka, B. Godin, R. Bhavane, R. Nieves-Alicea, J. Gu, X. Liu, C. Chiappini, J. R. Fakhoury, S. Amra, A. Ewing, Q. Li, I. J. Fidler and M. Ferrari, *International Journal of Pharmaceutics*, 2010, **402**, 190-197.
167.J.-H. Park, L. Gu, G. von Maltzahn, E. Ruoslahti, S. N. Bhatia and M. J. Sailor, *Nat Mater*, 2009, **8**, 331-336.
168.L. Cheng, E. Anglin, F. Cunin, D. Kim, M. J. Sailor, I. Falkenstein, A. Tammewar and W. R. Freeman, *Br J Ophthalmol.* , 2008, **92**, 705-711.
169.M. Sarparanta, E. Mäkilä, T. Heikkilä, J. Salonen, E. Kukk, V.-P. Lehto, H. A. Santos, J. Hirvonen and A. J. Airaksinen, *Molecular Pharmaceutics*, 2011, **8**, 1799-1806.
170.M. Sarparanta, L. M. Bimbo, J. Rytkönen, E. Mäkilä, T. J. Laaksonen, P. Laaksonen, M. Nyman, J. Salonen, M. B. Linder, J. Hirvonen, H. A. Santos and A. J. Airaksinen, *Molecular Pharmaceutics*, 2012, **9**, 654-663.
171.P. Decuzzi, B. Godin, T. Tanaka, S. Y. Lee, C. Chiappini, X. Liu and M. Ferrari, *Journal of Controlled Release*, 2010, **141**, 320-327.
172.J. Salonen, L. Laitinen, A. M. Kaukonen, J. Tuura, M. Björkqvist, T. Heikkilä, K. Vähä-Heikkilä, J. Hirvonen and V. P. Lehto, *J. Control. Release*, 2005, **108**, 362-374.
173.E. C. Wu, J.-H. Park, J. Park, E. Segal, F. d. r. Cunin and M. J. Sailor, *ACS Nano*, 2008, **2**, 2401-2409.
174.T. Limnell, J. Riikonen, J. Salonen, A. M. Kaukonen, L. Laitinen, J. Hirvonen and V. P. Lehto, *Int. J. Pharm.*, 2007, **343**, 141-147.
175.A. M. Kaukonen, L. Laitinen, J. Salonen, J. Tuura, T. Heikkilä, T. Limnell, J. Hirvonen and V.-P. Lehto, *Eur. J. Pharm. Biopharm.*, 2007, **66**, 348-356.
176.F. Wang, H. Hui, T. J. Barnes, C. Barnett and C. A. Prestidge, *Molecular Pharmaceutics*, 2009, **7**, 227-236.
177.E. C. Wu, J. S. Andrew, A. Buyanin, J. M. Kinsella and M. J. Sailor, *Chem. Commun.*, 2011.
178.P. Kinnari, E. Mäkilä, T. Heikkilä, J. Salonen, J. Hirvonen and H. A. Santos, *International Journal of Pharmaceutics*, 2011, **414**, 148-156.
179.A. P. Mann, T. Tanaka, A. Somasunderam, X. Liu, D. G. Gorenstein and M. Ferrari, *Adv. Mater.*, 2011, **23**, H278-H282.
180.S. Ferrati, A. Mack, C. Chiappini, X. Liu, A. J. Bean, M. Ferrari and R. E. Serda, *Nanoscale*, 2010, **2**, 1512-1520.
181.L. M. Bimbo, E. Mäkilä, T. Laaksonen, V.-P. Lehto, J. Salonen, J. Hirvonen and H. A. Santos, *Biomaterials*, 2011, **32**, 2625-2633.
182.L. M. Bimbo, E. Mäkilä, J. Raula, T. Laaksonen, P. Laaksonen, K. Strommer, E. I. Kauppinen, J. Salonen, M. B. Linder, J. Hirvonen and H. A. Santos, *Biomaterials*, 2011, **32**, 9089-9099.
183.L. M. Bimbo, M. Sarparanta, E. Makila, T. Laaksonen, P. Laaksonen, J. Salonen, M. B. Linder, J. Hirvonen, A. J. Airaksinen and H. A. Santos, *Nanoscale*, 2012, **4**, 3184-3192.
184.M. P. Sarparanta, L. M. Bimbo, E. M. Mäkilä, J. J. Salonen, P. H. Laaksonen, A. M. K. Helariutta, M. B. Linder, J. T. Hirvonen, T. J. Laaksonen, H. A. Santos and A. J. Airaksinen, *Biomaterials*, 2012, **33**, 3353-3362.
185.N. Vale, E. Mäkilä, J. Salonen, P. Gomes, J. Hirvonen and H. A. Santos, *European Journal of Pharmaceutics and Biopharmaceutics*.
186.T. Tanaka, L. S. Mangala, P. E. Vivas-Mejia, R. Nieves-Alicea, A. P. Mann, E. Mora, H.-D. Han, M. M. K. Shahzad, X. Liu, R. Bhavane, J. Gu, J. R. Fakhoury, C. Chiappini, C. Lu, K. Matsuo, B. Godin, R. L. Stone, A. M. Nick, G. Lopez-Berestein, A. K. Sood and M. Ferrari, *Cancer Res*, 2010, **70**, 3687-3696.
187.M. Kilpeläinen, J. Riikonen, M. A. Vlasova, A. Huotari, V. P. Lehto, J. Salonen, K. H. Herzig and K. Järvinen, *J. Control. Release*, 2009, **137**, 166-170.
188.M. Kilpeläinen, J. Mönkäre, M. A. Vlasova, J. Riikonen, V.-P. Lehto, J. Salonen, K. Järvinen and K.-H. Herzig, *European Journal of Pharmaceutics and Biopharmaceutics*, 2011, **77**, 20-25.
189.A. S.-W. Goh, A. Y.-F. Chung, R. H.-G. Lo, T.-N. Lau, S. W.-K. Yu, M. Chng, S. Satchithanantham, S. L.-E. Loong, D. C.-E. Ng, B.-C. Lim, S. Connor and P. K.-H. Chow, *Int. J. Radiation Oncology Biol. Phys.*, 2007, **67**, 786-792.
190.M. J. Sailor and J. R. Link, *Chem. Commun.*, 2005, 1375-1383.
191.L. Russo, F. Colangelo, R. Cioffi, I. Rea and L. D. Stefano, *Materials*, 2011, **4**, 1023-1033.
192.J. R. Link and M. J. Sailor, *Proc. Nat. Acad. Sci. U. S. A.*, 2003, **100**, 10607.
193.T. A. Schmedake, F. Cunin, J. R. Link and M. J. Sailor, *Adv. Mater.*, 2002, **14**, 1270-1272.
194.S. G. Kim, S. Kim, Y. C. Ko, S. Cho and H. Sohn, *Colloids Surfaces A*, 2008, **313-314**, 398-401.
195.F. Cunin, T. A. Schmedake, J. R. Link, Y. Y. Li, J. Koh, S. N. Bhatia and M. J. Sailor, *Nat Mater*, 2002, **1**, 39-41.
196.E. C. Wu, J. S. Andrew, L. Cheng, W. R. Freeman, L. Pearson and M. J. Sailor, *Biomaterials*, 2011, **32**, 1957-1966.
197.H. Cheng, X. Zhou, C. K. Tsang, J.-W. Cheng, F. Liang, B. Zheng and Y. Y. Li, *phys. stat. sol. (c)*, 2011, **8**, 1754-1758.
198.Y. Y. Li, F. Cunin, J. R. Link, T. Gao, R. E. Betts, S. H. Reiver, V. Chin, S. N. Bhatia and M. J. Sailor, *SCIENCE*, 2003, **299**, 2045-2047.
199.M. H. Cohen, K. Melnik, A. A. Boiarski, M. Ferrari and F. J. Martin, *Biomed. Microdevices*, 2003, **5**, 253-259.
200.C. Chiappini, E. Tasciotti, R. E. Serda, L. Brousseau, X. Liu and M. Ferrari, *physica status solidi (c)*, 2011, **8**, 1826-1832.
201.B. Godin, C. Chiappini, S. Srinivasan, J. F. Alexander, K. Yokoi, M. Ferrari, P. Decuzzi and X. Liu, *Advanced Functional Materials*, 2012, DOI: 10.1002/adfm.201200869.
202.G. Adriani, M. D. de Tullio, M. Ferrari, F. Hussain, G. Pascazio, X. Liu and P. Decuzzi, *Biomaterials*, 2012, **33**, 5504-5513.
203.J. R. Dorvee, A. M. Derfus, S. N. Bhatia and M. J. Sailor, *Nat Mater*, 2004, **3**, 896-899.
204.J.-H. Park, A. M. Derfus, E. Segal, K. S. Vecchio, S. N. Bhatia and M. J. Sailor, *J. Am. Chem. Soc.*, 2006, **128**, 7938-7946.
205.J. C. Thomas, C. Pacholski and M. J. Sailor, *Lab on a Chip*, 2006, **6**, 782-787.
206.L. Gu, J.-H. Park, K. H. Duong, E. Ruoslahti and M. J. Sailor, *Small*, 2010, **6**, 2546-2552.
207.Á. Muñoz-Noval, V. Sánchez-Vaquero, V. Torres-Costa, D. Gallach, V. Ferro-Llanos, J. J. Serrano, M. Manso-Silván, J. P. García-Ruiz, F. d. Pozo and R. J. Martín-Palma, *journal article*, 2011, **16**, 025002.

208.Á. Muñoz-Noval, V. Sánchez-Vaquero, V. Torres-Costa, D. Gallach, M. Manso-Silván, J. P. García-Ruiz, M. Hernando-Pérez, P. J. d. Pablo and R. J. Martín-Palma, *Silicon-based hybrid luminescent/magnetic porous nanoparticles for biomedical applications*, SPIE, 2011.

209.E. Tasciotti, X. Liu, R. Bhavane, K. Plant, A. D. Leonard, B. K. Price, M. M.-C. Cheng, P. Decuzzi, J. M. Tour, F. Robertson and M. Ferrari, *Nat Nano*, 2008, **3**, 151-157.

210.R. E. Serda, A. Mack, A. L. van de Ven, S. Ferrati, K. Dunner, B. Godin, C. Chiappini, M. Landry, L. Brousseau, X. Liu, A. J. Bean and M. Ferrari, *Small*, 2010, **6**, 2691-2700.